X-612-65-417

55387

# MAGNETIC STORMS IN THE EARTH'S MAGNETIC TAIL



BY

K. W. BEHANNON

AND

NORMAN F. NESS

OCTOBER 1965

NASA

GODDARD SPACE FLIGHT CENTER

GREENBELT, MARYLAND

X-612-65-417

# MAGNETIC STORMS IN THE EARTH'S MAGNETIC TAIL

by

K. W. Behannon

and

N. F. Ness

NASA-Goddard Space Flight Center

Greenbelt, Maryland

ABSTRACT

N66-18394

Detailed measurements of the earth's magnetic field at distances between 7 and 31.4 $R_E$ were obtained by the IMP-I satellite between November 27, 1963 and May 30, 1964. The interaction of the solar wind with the geomagnetic field compresses it on the sunlit hemisphere but extends the field to form a magnetic tail in the antisolar direction with a median magnitude of 16 gammas. From March 15 to June 3, 1964 the satellite was imbedded well within the magnetic tail and for 19+ orbits (29-48) measured principally the temporal variation and spatial structure of this tail field. The experimental data reveal the development of a magnetically neutral sheet in the tail separating fields of opposite direction which are aligned parallel to the earth-sun line. A total of 5 magnetic storms were observed terrestrially which are correlated with satellite data and discussed in this paper. Three storms of an M-region sequence, presumed to be associated with the sector structure within the corotating interplanetary medium are presented and discussed in detail, as well as two other magnetic storms.

Author

Both positive and negative correlations with world wide H-component terrestrial data are observed. The former is interpreted to be due to large scale compression of the entire magnetosphere and tail. Anticorrelation of the H-component with the tail field magnitude is shown to be due to an increased number of lines of force being carried into the tail by the enhanced solar plasma flow. This occurs simultaneous with the main phase decrease and thus supports geomagnetic storm theories invoking such a tail field mechanism. Positive correlations of an increased tail field magnitude with the planetary magnetic index Kp are also obtained.

TABLE OF CONTENTS

## INTRODUCTION

From November 27, 1963 to May 30, 1964 the IMP 1 satellite performed extensive measurements of the magnetic fields in space at distances greater than approximately 7 $R_E$ (Earth radii). The initial apogee of the satellite was on the sunlit side of the Earth at an Earth-Sun angle of approximately 25° west of the Sun and a geocentric distance of 197,616 kilometers = 31.7 $R_E$. The period of the highly eccentric orbit is 93.5 hours. In a geocentric solar ecliptic coordinate system the apparent motion of the satellite is one of westward precession of 4°/orbit as the Earth moves around the Sun.

On May 30 the operation of the spacecraft became intermittent, with the duration of on-times gradually decreasing. This behavior was due to battery degradation and an increasingly less favorable spin axis-Sun angle for power generation by the solar paddles. The cislunar region swept out by the satellite during the six-month period of continuous operation is shown in figure 1. A description of the instruments and initial results obtained from the 47 orbits of IMP 1 have been presented by Ness et al. (1964), Ness and Wilcox (1964), Ness (1965a, b); Ness and Wilcox (1965, 1966), Ness et al. (1965), Ness and Williams (1966) and Wilcox and Ness (1965).

Detailed mapping of the geomagnetic field in the dark hemisphere was obtained out to geocentric distances of 31.4 $R_E$ from the sunrise meridian to 25° east of the midnight meridian. This survey had the significant result of revealing the existence of an extended magnetic tail behind the Earth with a magnetically neutral sheet separating regions of opposite field direction (Ness, 1965b).

Measurements of the magnetic field in the Earth's tail by Explorer 14 have verified the existence of the neutral sheet (Cahill, 1965). Particle measurements by Anderson (1965a, b), Anderson et al. (1965), Freeman (1964), Gringauz et al. (1960), McDiarmid and Burrows (1965), Montgomery et al. (1965) and Singer et al. (1965) have found enhanced particle fluxes on the night side of the Earth. Certain of these are probably related to the neutral sheet (Axford et al., 1965). Particularly pertinent in this respect are measurements by Frank (1965) with the Explorer 14 satellite which revealed the formation of an "electron tail" of the magnetosphere.

Figure 2 shows the topology of the geomagnetic field and a sample IMP 1 orbit projected onto the noon-midnight meridian plane. The topology observed in the tail of the magnetosphere by IMP 1 is in agreement with the configuration discussed by Piddington (1960). An important contribution of the observations has been to show that the magnetic tail is a permanent feature of the distorted geomagnetic field in cislunar space. It is postulated that the magnetic field lines of the tail originate in the polar cap regions of the Earth's dipole field. Although the exact mechanism for the extension of field lines is not clear, Piddington (1959), Axford and Hines (1961), and Axford (1964) have suggested that it is due to the "viscous drag" of the solar wind on the magnetospheric boundary. The magnetic tail does not corotate with the Earth, although magnetic lines of force on the night side corresponding to L values of less than approximately 8 appear to corotate.

The Earth's magnetic tail is evidently a reservoir of energetic electrons and it is more than likely able to capture particles from the solar wind

(Fejer, 1965: Wentworth, 1965). The effects of variations in the solar plasma flux and/or an interaction between the terrestrial magnetic field and the interplanetary field can be expected to produce conditions conductive to acceleration of particles in the tail (Dessler and Walters, 1964; Piddington, 1964). This energizing of particles will increase as the interplanetary medium becomes increasingly disturbed or as conditions there become more favorable for coupling with the Earth's magnetic field. Thus the tail may play a dominant role in various terrestrial phenomena. The day-night asymmetry observed in many of these phenomena, including certain of the geomagnetic field variations and auroral activity, would seem to support this view.

It is the purpose of the present paper to present observational data relating tail activity and characteristics during storm times to terrestrial magnetic phenomena. This evidence consists of correlations between the magnetic field variations observed in the tail, the 3-hourly planetary magnetic activity index Kp, and the H-component of the geomagnetic field at a number of observatories. Special emphasis is placed on 5 separate periods of geomagnetic disturbance, 3 of which belong to the same family of M-region disturbances. Examples of detailed correlation between storm-time tail field variation and polar substorm activity will be presented in a separate paper.

## SOLAR AND GEOMAGNETIC ACTIVITY

The IMP-1 spacecraft was located within the tail of the magnetosphere during the 81-day period from March 15 to June 3, 1964 corresponding to orbits 29-48. It will be necessary first to review the solar and geomagnetic activity of that period in order to provide a meaningful interpretation for the magnetic field variations seen by the satellite. The following summary was prepared from information compiled and published by the National Bureau of Standards (Boulder High Altitude Observatory, 1964; Central Radio Propagation Laboratory, 1964). Sudden commencement (SC) times given are mean values obtained from normal magnetograms (Lincoln, 1965a, b).

On March 16 a class 2+ flare was observed both optically and electronically in connection with major radio bursts and in association with plages 7182 and 7187. A moderate geomagnetic disturbance occurred on March 21 with SC at 1950 UT (SC: 9 stations, SI: 5 stations). The maximum value of the 3-hourly planetary magnetic activity index Kp for this storm was 6o on March 23. On March 22 the sunspot number ($R_A$) was 32, the highest for this 81-day period (the yearly mean for 1964 was 10.2). Also on March 22 a region of extremely strong 5303A coronal emission had its central meridian passage (CMP) along with plage 7187.

Radio noise storms were detected during March 22-24, and minor flares were observed on March 23 and 25 in association with plage 7189. Another extremely strong 5303A region crossed central median on March 28, along with plage 7192. A moderate geomagnetic disturbance began on March 29, with an SC at 1408 UT (SC: 24 stations, SI: 8 stations). A moderately severe

storm with an SC at 1525 UT (SC: 4 stations) on April 1 ended at 05XX UT on April 3. Kp reached a maximum value of 7+ on April 1. This was the highest value seen during this 81-day period. As it was preceded by a storm 27 days before, it was classified as the second disturbance in an M-region sequence.

On April 5 a strong 5303A region had its CMP. There were no coronal observations during April 6-14. A class 3 flare was observed on April 7 and a geomagnetic disturbance with SC at 0808 UT (SC: 4 stations, SI: 2 stations) was reported for April 8. There was further minor flare activity during April 9-13. Eastern limb surges on April 10 and 11 preceded the reappearance of plage region 7224 (7187 on the previous rotation). Boulder suggested that the more frequent appearance of high latitude plages, features of the new solar cycle, was indicative of passage through solar minimum.

A geomagnetic disturbance with SC at 1625 UT (SC: 23 stations, SI: 8 stations) began on April 13, and another moderate disturbance commenced on April 17 with SC at 0020 UT (SC: 31 stations, SI: 5 stations). On April 18 a strong 5303A region had its CMP along with plages 7224 and 7236. There were no coronal observations on April 20 or during April 23-30. A moderately severe storm, third in an M-region sequence, began on April 27 at 14XX UT and ended at 21XX UT on April 29. Highest Kp for this storm was 5+.

Plage 7269 had its CMP on May 4, and plage 7264 followed on May 7. On May 10 an SC storm of moderate intensity began at 0035 UT (SC: 63 stations) and had a maximum Kp of 5+ on May 11. It was followed on May 13 by another moderate disturbance which began at 1301 UT (SC: 17 stations, SI: 11 stations) and ended at 23XX UT on May 16. Kp reached a maximum value of 6o on May 15.

Boulder reported this storm to be one of a sequence of enhanced values at approximately 27-day intervals dating back to July, 1963.

There were no coronal observations during May 11-16 or May 19-21. Class 2 flares were observed on May 21 and 22 following minor flare activity on May 18 and 20 in association with plages 7279 and 7286. A moderately severe geomagnetic storm with SC at 2229 UT (SC: 62 stations) began on May 23 and ended at 01XX UT on May 26. It was the fourth in the M-region sequence that included the April 1 and April 27 storms.

## CONDITION OF THE INTERPLANETARY MEDIUM

Much effort has been expended trying to relate geomagnetic disturbances to active regions on the sun where one observes the rise, development, and subsequent disappearance of intense magnetic fields, faculae, sunspots, chromospheric flares, disturbed coronal regions, and prominences. It was asserted some time ago (Allen, 1944) that there could be a division of storms into two classes depending on their characteristics and most probably on the mechanism producing them. One class includes intense storms that have sudden commencements, can be associated with sunspots, follow bright chromospheric eruptions after about a day and have no 27-day recurrence.

Storms of the other class are not as intense, do not seem to be directly related to visible solar features, and tend to recur after 27 days. It was seen even then that it was extremely difficult to assign individual storms to one class or the other with certainty and that there were many exceptions in regard to the various features of each of the two classes.

The statistical relation of non-recurrent geomagnetic activity to significant solar flares, dependent on the heliographic location of the flares, has been amply demonstrated (Newton, 1944; Bell, 1962; Jenkins and Paghis, 1963). Finding an explanation for the recurrent storms has not been quite so straightforward. For want of a specific mechanism they were attributed to hypothetical "M-regions" on the Sun (Bartels, 1932). Statistical studies (Allen, 1944; Saemundsson, 1962) indicated that M-regions tend to avoid the immediate vicinity of active solar areas but are strengthened just outside these areas,

especially on the following side. A "cone of avoidance" hypothesis (Pecker and Roberts, 1955) suggested that such cones are created above active regions with an intensification of corpuscular emission at the boundaries of the cones.

Simpson and the Babcocks (1955) reported that on seven consecutive rotations of the Sun in 1953 there was a striking association of a unipolar solar magnetic field region (UMR) with cosmic ray intensity changes as well as with a series of recurring geomagnetic storms. Maximum disturbances occurred approximately four days after CMP of a UMR.

Subsequent theoretical studies led to various pictures of structuring in the interplanetary medium. Influencing these views was the knowledge of a complicated ray structure of the solar corona that had emerged from optical and radio astronomical observations. It was seen (Parker, 1958) that the large predominance of kinetic energy density of solar plasma streaming away from the Sun over the magnetic energy density of the gas would result in "frozen-in" lines of force and hence an "archimedes spiral" geometry for the interplanetary magnetic field due to the Sun's rotation.

After considering all the various possible components of a quasi-stationary emission of gases from the Sun, Mustel (1964) concluded that recurrent storms could be due to approximately radial streams of enhanced corpuscular flow originating from active regions which pass near the center of the solar disk, with the local magnetic field governing both the formation of the active region and the particle stream leaving that region. He asserts that the properties of the streams under consideration do not depend on the presence of sunspots and quiet prominence filaments in active regions.

He further claims that the greater density and magnetic field strength in the solar corona over active regions is an argument against the cone of avoidance hypothesis. Allen (1964) insists, however, that when the outward wind is strong and the magnetic field weak, the lines of force will be stretched out, whereas when the solar field is strong the solar plasma in these areas will be constrained by the field. He suggests that coronal streamers and UM regions are both likely features of M-regions.

Allen states that there are two possible interpretations of the statistical results. The A-interpretation, which he favors, requires the avoidance of a center of activity by an M-region and leads to a 3-day travel time for the disturbance particles, implying a mean velocity of 580 km/sec. The B-interpretation, as favored by Mustel, requires radial emission from a center of activity leading to a 6-day passage time and hence a mean velocity of 290 km/sec.

Others have begun to consider an M-region to be a feature of the interplanetary medium itself. Dessler and Fejer (1963) argue against the injection of an enhanced beam of solar plasma as causing the M-region storms because of the narrowness of the streams responsible for these disturbances. They suggest that recurrent geomagnetic disturbances are due to sheets of turbulence or irregularities that are generated at the interface of two solar wind regions of different stream velocities. The longitudinal local gradient in coronal heating may result in such a velocity discontinuity, and this band of irregularities would corotate with the Sun. They then suggest interpretation of Kp as a measure

of the time rate of change of the sum of plasma plus magnetic pressure acting on the magnetosphere.

Piddington (1964) has taken the view that recurrent storms are mainly due to a frictional interaction. When the interplanetary field is perpendicular to the geomagnetic field in the surface layer, friction is inhibited; when the fields are parallel (or the interplanetary field is very small), friction is not inhibited. Thus the field and plasma above an active region tend to sweep away irregular fields ahead and leave a region where the interplanetary field is weak or else nearly perpendicular to the geomagnetic equatorial plane. This region would constitute the M-region responsible for geomagnetic activity.

A theory similar to the preceding ones (Sarabhai, 1964) envisions a shock front between a region of enhanced plasma and the slow normal plasma being pushed ahead of it. It also proposes a cavity region on the trailing edge of the fast plasma due to slower plasma behind not being able to fill in the void. Total Kp > 25 and increases in the daily mean intensity of galactic cosmic rays are associated with CMP 3-4 days earlier of the trailing edge of a bright coronal zone of 5303A emission. The theory thus suggests that high Kp is caused by two distinct types of interplanetary conditions, (1) the passage of a corotating shock front or radially advancing blast wave and (2) the emergence of the Earth from a cavity.

Monitoring of the interplanetary medium by the IMP 1 satellite over a period of almost three months (November 27, 1963 - February 15, 1964) produced very revealing information concerning the characteristics of the interplanetary magnetic field (Ness et al., 1964) and the solar wind (Bridge et al.,

1965) during this period. A detailed analysis of these IMP 1 interplanetary data (Ness and Wilcox, 1964; Wilcox and Ness, 1965) showed a good correlation between photospheric and interplanetary field directions on a large scale and revealed a tendency for the interplanetary medium to be ordered into quasi-stationary sectors.

Within each sector there is an average magnetic field direction that is either toward the Sun or away from it at the Archimedes spiral angle. A sector boundary is defined by a 180° reversal of the field. In the leading portion of the sectors the interplanetary magnetic field magnitude, solar wind velocity, and corresponding geomagnetic activity tend to be large, while in the trailing portion of the sectors these quantities tend to be small. The plasma density is large in the preceding and trailing portions of the sectors and is small in the middle. Cosmic ray intensity is smaller in the preceding portion where the interplanetary field magnitude is larger, with conditions reversed in the trailing portion.

These conclusions agree with previous experimental results (Snyder et al., 1963) which found a close association of M-region storms with plasma velocity and a strong correlation between this velocity and Kp. Gringauz (1961) reports that Lunik II saw an increase in solar plasma flux at the time a geomagnetic storm began, and Scherb (1964) reports that Explorer 10 saw a shift to higher plasma energy and flux during a magnetic storm.

An average peak velocity of near 350 km/sec was seen in the sectors probed by IMP 1, corresponding to a transit time of 5 days and in close agreement with Mustel's B-interpretation. Individual values of the bulk velocity

ranged from 250 km/sec to 440 km/sec (Bridge et al., 1965), however, and an average velocity of 504 km/sec was obtained for the four months (August 29, 1962 - January 3, 1963) of the Mariner 2 experiment (Snyder et al., 1963). Hence there are periods when much shorter transit times are seen.

One of the recurring geomagnetic storms of the IMP 1 interplanetary period could be associated with a feature of the photospheric magnetic field (Wilcox and Ness, 1965) known as a ghost UMR (Bumba and Howard, 1965). Positive identification of the solar source of the interplanetary sector features still awaits additional observations, however.

Although there is still uncertainty concerning the generating mechanism for sector features, that some magnetically-modulated solar activity results in a structuring of the interplanetary medium is now an established fact. An extrapolation of the sector boundaries of the IMP 1 interplanetary data period (November 27, 1963 - February 15, 1964) to the period during which measurements were made in the magnetospheric tail (March 15 - June 3, 1964) is shown in figure 3.

In addition to the planetary magnetic activity index Kp, an approximate mean squared deviation field $\delta^2_{ST}$ for world wide disturbance as well as $D_{ST}$ has been computed. Digitized data for the horizontal component of the terrestrial magnetic field at 2.5 minute intervals have been processed using numerical filter procedures (Behannon and Ness, 1965). Hourly averages of the H-component at 9 low latitude stations (see Table I) were obtained from these data by use of a 25 point low-pass Chebyshev filter. That is, the average field

is defined as

$$\bar{H} = \sum_{i=1}^{25} W_i^{LP} H_i \qquad (1)$$

where the particular values of $W_i^{LP}$, when Fourier transformed, lead to an optimumly flat low pass filter, eliminating fluctuations with periods shorter than 2 hours. These hourly averages were then band-pass filtered to remove the first five harmonics of the daily periodic fluctuation and leave the residual long term and transient storm time variations at each station. Also individual station RMS deviation fields at hourly intervals were obtained from the 2.5 minute data as:

$$\delta = \sqrt{\frac{1}{N}\sum_{i=1}^{25}(H_i - \bar{H})^2} \qquad (2)$$

For the individual geomagnetic storms discussed later in this paper, the separate $\delta$ and D traces for each station are presented.

The data shown in Figure 3 represent a world wide average of the 9 stations (indicated by an asterisk, *) in Table I. The averages were computed so as to avoid preferentially weighting any particular longitude because of the non-uniform distribution of stations. It is observed from Table I that Kakioka and Guam are grouped around geomagnetic longitude $\Lambda = 210°$ and Moca and Hermanus near $\Lambda = 79°$. Thus these two sets of stations are separated by slightly over 120° in longitude. The center of the remaining 5 stations, Honolulu - Tucson

and Fredricksburg - San Juan - Huancayo is approximately at $\Lambda = 310°$ which is almost 120° from both the previous two groups. These considerations define the relative weights assigned to each of the stations, as shown in Table I, which are used in computing $\delta_{ST}$ and also $D_{ST}$. Note that the station data for D was multiplied by secant $\Phi$ (the geomagnetic latitude) in order to normalize the data to the equator.

The use of these numerical procedures permits the comparison of satellite data with ground data that has been analyzed by a uniform method and which yields a quantitative estimate of the energy ($\delta^2_{ST}$) in the disturbance field for the shorter period fluctuations. (In the interpretation of the individual storm events, reference is made to local time for the stations, which is shown for 00-06-12-18 hours UT in Figure 4.) It appears that the quantitative value $\delta^2_{ST}$ is a more useful parameter measuring the fluctuations of the terrestrial field than the traditional planetary index Kp.

From figure 3 it is obvious that the earlier sector pattern has undergone evolution in which some of the boundaries have shifted in time, possibly due to changes in average plasma velocity. Also some of the boundaries are seen to weaken and even to disappear at times, indicative of fluctuations in the source regions on the Sun. In spite of these changes a strong suggestion of the earlier pattern still remains. In reviewing the geomagnetic activity during the time period under consideration it was seen that most of the significant disturbances were of the recurrent or M-region class, although one might be able to associate some of these disturbances with visibly active regions on the Sun, especially the April 1 storm. A study of the daily average cosmic ray counts

(Central Radio Propagation Lab, 1964) shows evidence of the cosmic ray intensity behavior found to be characteristic of the sectors studied during the earlier period. This is especially true of the sector that is responsible for the April 1, April 27 and May 23 storms.

Thus one may make some assumptions about conditions in the interplanetary medium during most of the storms under consideration here, based on the activity pattern found within the sectors during the earlier period and on the results of the other interplanetary experiments previously discussed. It will be assumed that the maximum Kp during a storm is approximately coincident in time with the maximum solar wind velocity and interplanetary magnetic field magnitude. It will also be assumed that a peak in solar wind density and a 180° shift in the interplanetary field direction precede the onset of recurrent geomagnetic disturbances. It remains now to discuss the morphology of the significant disturbances occurring while the IMP 1 satellite was monitoring activity in the Earth's magnetic tail.

TABLE I

Geographic and Geomagnetic Coordinates of Magnetic Observatories and Their Local Time Differences From UT

| Observatory | Geographic | | Geomagnetic | | $\Delta T$ | Relative Weights |
|---|---|---|---|---|---|---|
| | $\phi$ | $\lambda$ | $\Phi$ | $\Lambda$ | | |
| CO College | N64° 52' | W147° 50' | 64.6° | 256.5° | $-9^h51^m20^s$ | not used |
| VI Victoria | N48° 31' | W123° 25' | 54.1° | 293.0° | $-8^h13^m40^s$ | not used |
| FR Fredricksburg* | N38° 12' | W77° 22' | 49.6° | 349.8° | $-5^h09^m28^s$ | 1/27 |
| KA Kakioka* | N36° 14' | E140° 11' | 26.0° | 206.0° | $+9^h20^m44^s$ | 1/6 |
| TU Tucson* | N32° 15' | W110° 50' | 40.4° | 312.2° | $-7^h23^m20^s$ | 1/9 |
| HO Honolulu* | N21° 19' | W158° 00' | 21.0° | 266.4° | $-10^h32^m0^s$ | 1/9 |
| SJ San Juan* | N18° 23' | W66° 07' | 29.9° | 3.2° | $-4^h24^m28^s$ | 1/27 |
| GU Guam* | N13° 35' | E144° 52' | 4.0° | 212.9° | $+9^h39^m28^s$ | 1/6 |
| MC Moca* | N3° 21' | E8° 40' | 5.7° | 78.6° | $+0^h34^m40^s$ | 1/6 |
| HU Huancayo* | S12° 03' | W75° 20' | - 0.6° | 353.8° | $-5^h1^m20^s$ | 1/27 |
| HR Hermanus* | S34° 25' | E19° 14' | -33.3° | 80.3° | $+1^h16^m56^s$ | 1/6 |

## PRESENTATION OF OBSERVATIONAL RESULTS

The primary objective of this study is to compare magnetic field time variations observed in the Earth's tail with variations in the surface field at a number of widely distributed low latitude magnetic observatories. An effective correlation of storm time variations can be made between satellite measurements and magnetic observatory measurements only if the latter data are processed in such a way as to remove the significant harmonics of the diurnal variations. Thus the procedures discussed previously were applied separately to the individual stations.

It is also important in studying geomagnetic field variations with a satellite experiment to distinguish as well as possible between purely spatial and purely temporal variations. To that end various spacecraft orbital parameters of value in isolating spatial effects have been plotted for the time periods of interest to this study. These parameters are defined as follows:

$\chi_{SS}$ - Geomagnetic latitude of the subsolar point. (A measure of the "angle of attack" of the solar wind.)

MLAT - Geomagnetic latitude of the subsatellite point.

RAD - Geocentric distance of the satellite in units of Earth radii ($R_E$).

$Z_{sm}$ - Perpendicular distance in $R_E$ from the XY-plane of the solar magnetospheric coordinate system. This right-hand system is defined such that $X_{sm}$ always points toward the Sun, the $Z_{sm}$ axis is directed so that the $X_{sm}$ - $Z_{sm}$ plane always includes

the geomagnetic dipole axis, and $Y_{sm}$ is always orthogonal to both the Earth-Sun line and the dipole axis. (Compare with solar ecliptic coordinate system used in studies of the interplanetary medium, Ness (1965b).)

$\theta_{sm}$ - Solar magnetospheric latitude of the subsatellite point.

Figure 5 shows $\chi_{ss}$ (solid line), $\theta_{sm}$ (dashed), and $Z_{sm}$ (dotted) for the period March 15 - May 28, 1964. When the actual orbital motion of the satellite is modulated by the daily "roll" of the $X_{sm}$ - $Y_{sm}$ plane, the result is the apparent motion described by $Z_{sm}$ and $\theta_{sm}$. Besides the diurnal variation in $\chi_{ss}$ one also sees the gradual seasonal shift of the subsolar point to more northerly geomagnetic latitudes. Meanwhile, in the progression from vernal equinox to summer solstice, the daily mean $X_{sm}$ - $Y_{sm}$ plane is gradually rotated into the ecliptic plane. Because of this the spacecraft is seen to spend increasingly more time above the $X_{sm}$ - $Y_{sm}$ plane. The significance of the solar magnetospheric equatorial plane lies in the fact that the neutral sheet of the magnetic tail is found to be located more nearly in this plane than in that defined by any other meaningful coordinate system (Ness, 1965b). The vertical lines in figure 7 identify neutral sheet crossings.

The geometry of the IMP 1 orbit is such that the satellite spends more than three days out of each 4-day orbit at values of RAD > 10 $R_E$. As may be seen from figure 2, the spacecraft was in the magnetic tail when beyond a distance of 10 $R_E$. It is also seen that the satellite is well below the ecliptic plane during the outbound portion of each orbit and through apogee.

Figures 6-11 show for the 81-day period of interest the planetary index Kp, the magnitude of the tail field $\overline{F}$, and the filtered hourly average H-components and RMS deviations of the H-components from the hourly averages at seven magnetic observatories. These data have been divided into successive 27-day intervals to facilitate the study of recurrent variations. One orbit in each interval is numbered to allow identification of all orbits. Geomagnetic disturbance commencement times have been included in the figures.

The high values at the ends of each orbital segment of tail field magnitude $\overline{F}$ are spatial features due to the rapid decrease and increase in magnetic field magnitude as the satellite goes out from and comes in toward perigee through the near-Earth field. The more gradual declines in $\overline{F}$ when outbound and steep increases inbound are due to the differences in geomagnetic latitude of the spacecraft and the variation of the magnetic flux density within the nightside magnetosphere. During orbits 29 and 30 the satellite's trajectory carried it outside the magnetospheric boundary and the data from those periods have been omitted. On May 6 during orbit 42 IMP 1 was eclipsed by the Earth while near apogee. This extended shadow period caused the spacecraft to turn off temporarily.

In studying figures 6-11, one cannot fail to notice the high degree of correlation between $\overline{F}$ and Kp. This means that $\overline{F}$ generally anticorrelates with the local D field storm variations. It is seen that each time a main phase decrease commences on the ground, $\overline{F}$ begins to increase toward a maximum value. It has been suggested (Axford et al., 1965) that at least a part of the depression of the main dipole field of the earth in equatorial regions during

magnetic storms could be due to the effect of a neutral sheet field, $H_T$. The magnitude of $H_T$ in equatorial regions would be roughly the same as in the tail and the direction would be opposite to that of the dipole field.

Figure 12 shows the distribution of tail field magnitude during the period under study. The median magnitude was 16 gammas, and values as high as 40 gammas were seen only during times of greatest disturbance (part of the tail on the high magnitude end of the distribution is due to a spatial rather than a temporal increase in magnitude). For the moderate storms of this period the tail field magnitude maxima were found to lie in the 25-35 gamma range. Since low latitude main phase decreases of approximately 100 gammas were seen during several of the storms under discussion, the IMP 1 tail field measurements show that the major part of the main phase decrease must be due either to some mechanism other than a neutral sheet field or a more complex or non-linear relationship between the tail field and $D_{ST}$ field must exist.

The local RMS deviations all correlate quite well with Kp with roughly the same time structure and are seen generally to decrease in magnitude toward the magnetic equator. The "spicular" character of these deviations emphasizes that the disturbance energy input process is an impulsive and fluctuating one, especially at the higher latitudes.

Five magnetic storms were selected for more detailed study. Three of them (April 1, April 27 and May 23) were well-defined members of an M-region sequence. The May 10 disturbance was the best example in this period of the classical SC storm. It was followed closely by a disturbance

(May 13) which also appeared to be a member of a long-lived recurrent sequence. Of the three storms in that sequence which occurred during the period under consideration, it is the one for which the longest run of $\overline{F}$ data was obtained. Unfortunately, the May 23 disturbance commenced while IMP 1 was at perigee, but since the storm was a complex and prolonged one, there was still a significant degree of activity in the tail field when the satellite once again reached that region of the Earth's magnetic environment.

The field variations seen at high latitude during these five geomagnetic storms are shown for College, Alaska, in figure 13. Figures 14-27 show the IMP 1 trajectory parameters $\chi_{SS}$, MLAT, RAD and $Z_{SM}$; the tail field magnitude $\overline{F}$; the angle $\theta$ between the tail field vector and the ecliptic plane; the angle $\phi$ between the Earth-Sun line and the projection of the tail field vector onto the ecliptic plane; and the lower latitude disturbance field variations for these five storms.

The first of the selected magnetic storms was the 1525 UT storm of April 1. It was a recurrent storm and yet it was preceded by a period of visible solar activity. Figure 14 shows the trajectory parameters for three days (March 31 - April 2) of orbit no. 33. It is seen that the satellite should have been well below the neutral sheet and near apogee when the disturbance commenced.

From figure 15 it is seen that the 12 hours preceding the commencement were characterized by wide fluctuations in $\overline{F}$ and $\theta$ and, to a lesser degree, in $\phi$. This field fluctuation has a period of approximately three hours and continues for four cycles before the large magnitude increase at storm commencement. This variation does not appear to be accompanied by any significant

activity on the ground at either high or low latitudes. It may represent a slow "fluttering" of the tail in which the neutral sheet is periodically brought nearer to the spacecraft with accompanying decrease in $\overline{F}$ and increase of $\theta$ toward 90°. $Z_{sm}$ shows that the neutral sheet was tilting toward the satellite at that time. It may also be that the neutral sheet is thicker near the flanks of the magnetic tail than the approximately few tenths $R_E$ seen during several traversals nearer the noon-midnight meridian plane (Ness, 1965). A thickening of the sheet nearer the Earth was seen by Explorer 14 (Cahill, 1965) in agreement with the theoretical picture drawn by Axford et al. (1965). A tubular "bundling" of the lines of force drawn back into the tail from each of the magnetic poles would result in a thickening of the sheet toward the flanks also.

The tail field magnitude is seen to increase to more than twice its pre-storm level and to remain high during most of the period of H-component depression. Just prior to the SC time it increases to approximately 17 gammas in about 20 minutes. Some of the surface local storm fields, including that at College, which had been decreasing for several hours before this time, experienced temporary increases coincident with the large and rapid increase in $\overline{F}$. Following the SC time they all begin to decline again.

After being approximately 35 gammas for about two hours $\overline{F}$ undergoes a temporary, bay-like decrease, reaching a minimum of about 22 gammas at approximately 1800 UT. This coincides with the first low point seen in the low latitude disturbance fields and also the minimum of the first large negative bay seen at College and other high latitude observatories. As $\overline{F}$ recovers to its previous enhanced level a partial recovery is also seen in the H-components at

all latitudes, with higher latitude fields experiencing a more nearly complete recovery.

During the next three hours the tail field declines somewhat and fluctuates widely in magnitude and direction. At this time the H-component minimum occurs at some of the low latitude stations and a second substorm is seen at high latitudes, being most intense in the evening quadrant.

At approximately 2300 UT a maximum value of near 40 gammas is reached by $\overline{F}$. Shortly after this it begins to decline. Perhaps this is in part due to a temporal decrease, but the trajectory parameters indicate that the satellite is again approaching the neutral sheet at this time. Still, Kp is decreasing during the first 12 hours of April 2 so that one expects this decline in geomagnetic activity to be reflected in the behavior of $\overline{F}$. The behavior of the tail field magnitude and direction during the eight hours centered around 1200 UT on April 2 strongly suggests proximity to but not complete traversal of the neutral sheet. The field fluctuations seen at this time are indicative of either a fluttering of the tail or some sort of activity in or near the neutral sheet. Low latitude surface fields are somewhat irregular at this time and another substorm of approximately 600 gammas is seen at College.

It was during this storm that the APL satellite 1963 38C was sampling the trapped electron population at an altitude of 1100 km while IMP 1 was measuring tail field variations (Ness and Williams, 1965). Passes made prior to the disturbance display quiet-time profiles. Measurements made at 0000 UT April 2 show a distinct collapse of the outer trapping boundary to lower

latitudes. The next pass at 0526 UT showed that the outer boundary had moved back to its prestorm value and that new particles had been added.

The tail field data for this disturbance are presented on an expanded time scale in figures 16-18. These data extend over three orbits and hence cover most of the recovery phase of this storm as well as the small 0808 UT disturbance on April 8. The dashed lines show the field predicted by the Finch and Leaton Coefficients (Finch and Leaton, 1957) for a spherical harmonic representation of the Earth's field.

As the spacecraft moves in toward the Earth on orbit 33 the tail field magnitude is seen to increase to slightly more than 40 gammas at 12 $R_E$ and then fall to very low values at about 10 $R_E$ as the neutral sheet is finally traversed at the near-Earth end. During orbit 34 the tail field is seen to have settled down to what is probably near quiet tail conditions, with the magnitude $\overline{F}$ down around its median value of 16 gammas at apogee. The variations seen after 0000 UT on April 6 are again most probably due to the satellite being periodically immersed in the neutral sheet by tail fluctuations.

The first interesting point concerning the outbound portion of orbit 35, as shown by figure 18, is that the tail field magnitude at 20 $R_E$ is some 20 gammas higher than it was during the outbound portion of orbit 33. That time in orbit 33 was early in the recovery phase of the disturbance that commenced at 1408 UT on March 29. However, figure 6 shows that Kp had decreased to 0+ rather abruptly at that time, indicating an almost immediate cessation of geomagnetic disturbance, whereas at the time that the spacecraft is at 20 $R_E$

in orbit 35, a Kp of 3+ is seen. After having fallen off gradually during the recovery phase of the April 1 storm, the planetary index had become enhanced to values just below the storm level beginning in the last three hours of April 6 and is seen to reach a value of 4o just after commencement of the April 8 disturbance.

$\overline{F}$ is seen to decrease to approximately 20 gammas as the satellite continues outbound. Then at a distance of about 29 $R_E$, following the onset of this relatively minor storm, a maximum magnitude of 25 gammas is observed. At 10 $R_E$ inbound on orbit 35 Kp is the lowest that it has been at that distance during the three orbits, and in figure 18 it is seen that the least depression of $\overline{F}$ and most gradual swing-around of $\phi$ occur at that time. This is consistent with the Explorer 14 results (Cahill, 1965) in which an apparent compression of the neutral sheet was seen during a time of geomagnetic disturbance. Also the near-Earth end of the sheet may be drawn further away from the Earth during quiet times, so that during orbit 35 the less pronounced depression of $\overline{F}$ observed at 10 $R_E$ could have been due more to the effect of the plasma pocket seen just outside the stable trapping region by Gringauz et al. (1960) and Freeman (1964) and discussed by Cahill (1965).

The position parameters of IMP-1 for the geomagnetic disturbance commencing at 14XX UT on April 27 are shown in figure 19. This storm, shown in Figure 20, represents the return of the interplanetary medium sector region responsible for the April 1 storm, and is characterized more by widely fluctuating fields than by any simple pattern of main phase decrease followed by smooth and steady recovery. It is seen that the tail field magnitude was already

somewhat enhanced prior to the storm. However, it increased even more to a maximum of about 36 gammas following commencement of the storm.

On the ground the low latitude stations of Moca and Hermanus with local times in the early evening show the most regular H-component decrease. College experiences a substorm prior to the storm commencement time, and an even deeper decrease is seen following that time. This maximum depression of the surface field at Moca, Hermanus and College anticorrelates with $\overline{F}$ during the 10-hour period following the commencement.

$\overline{F}$ is seen to fluctuate widely throughout the first half of April 28 and then to smooth out during the next 12 hours. This same pattern of activity is seen at the low latitude observatories and at College, where an extended period of substorm activity abruptly ceases at about 1400 UT and is followed by relatively quiet conditions for the remainder of the day. IMP 1 nears the neutral sheet on the following day, and finally passes through it just before midnight UT. Meanwhile a number of sharp decreases of about 10 gammas are seen in the $\overline{F}$ data. Some of these very distinctive changes in $\overline{F}$ are seen to be accompanied by features in the local D fields which seem to be dependent on local time for their form. Correlation with $\overline{F}$ during these rapid decreases has been found in the H-components at several night-time polar stations.

Some of the sudden decreases seen in $\overline{F}$ on April 29 have been correlated with precipitous increases in particle fluxes (Ness et al., 1965). Such particle fluxes seen in the tail by IMP 1 have been termed "electron islands" (Anderson et al., 1965) because of their rather narrow temporal extent. A total of 126

energetic electron islands have peak flux > $10^5$ $cm^{-2}$ $sec^{-1}$ were seen during 17 orbits through the tail region. They were found to exhibit a fast-rise, slow-decay characteristic suggesting that they were impulsively injected into a region of space much more rapidly than the spacecraft moved through that region. The decay of the flux was often found to be roughly exponential, suggesting depletion of the source region. The relative frequency of appearance of electron fluxes above 45 keV was found to rapidly decrease with radial distance in the tail.

The correlated electron flux and tail field magnitude variations on April 29 are shown in figure 21. The close proximity of the spacecraft to the neutral sheet at this time strongly suggests that the neutral sheet is the source of these particles. That large transient variations are seen in surface field magnitudes at the times of these particle events, especially at 0100 UT and 1800 UT, adds further emphasis to the possibility that the Earth's tail is intimately involved in terrestrial magnetic disturbances. It indicates that the disturbance-producing mechanisms influence events throughout a larger volume of space than was once supposed.

As mentioned previously, the May 10 geomagnetic disturbance is the most typical of the ideal sudden commencement storm that was seen during the period under study. Figure 22 shows that the neutral sheet was encountered on the second day of the storm. However, it was far enough away from the sheet throughout most of the April 1 event, to give a good picture of events in the tail field during the commencement, initial phase, and the onset of the main phase.

From figures 13 and 23 it is seen that the SC impulse was seen at all latitudes on the ground as well as at a distance from the earth of around 31 $R_E$ near the noon-midnight meridian plane. Other impulsive features are seen both on the surface and in the tail during the initial phase of the storm, implying successive perturbations of the entire magnetosphere by structures in the enhanced solar plasma stream.

The increase to a sustained high value for $\overline{F}$ is seen to occur around 1100 UT. All of the low latitude stations, especially Moca near local noon, show a small rise in H-component magnitude at that time. The field is seen to increase gradually at College until at approximately 1230 UT it drops abruptly with the onset of a substorm. There is a 15 gamma negative spike in $\overline{F}$ at this time, and the main phase decrease begins at low latitudes.

During the main phase decline an anticorrelation is seen between detailed features in $\overline{F}$ and in the H-component at Victoria. After $\overline{F}$ reaches a maximum of about 34 gammas it is seen to gradually decline in trend even as many of the low latitude local D fields are continuing to decrease toward their minimum values. Victoria reaches a minimum early and then briefly recovers to the initial phase level at 0000 UT before dropping again to a value that is even lower than the previous minimum. Magnetic activity at College follows roughly the same pattern except that the second negative bay is much weaker than the first.

The declining tendency of $\overline{F}$ in the latter part of May 10 may be due in part to the spatial effect of a gradual weakening of the tail field near the neutral sheet. One observes a gradual increase in $\theta$ throughout May 10. Then at

about 0100 UT on May 11 actual penetration of the sheet is signaled by a sudden 12 gamma drop in $\overline{F}$ accompanied by large excursions in $\theta$ and $\phi$.

From the general behavior of the tail field at the position of the satellite during the next 12 hours, it appears that the spacecraft, which was initially east of the noon-midnight meridian plane, was moving along close beneath the neutral sheet and overtook it while it was tilting to the west. The relative motion is such that IMP 1 remains in the sheet for a significant period of time, although the neutral sheet appears to oscillate between positions above and below the satellite. Finally as the spacecraft continues on toward the Earth on the western side of the noon-midnight meridian plane, the neutral sheet is seen to move above IMP 1 as the sheet tilts back toward the east.

The May 13 disturbance (Figures 24 and 25) is another one that is characterized mostly by a high degree of field irregularity or turbulence. As in the case of the April 27 storm one sees an anticorrelation between $\overline{F}$ and the local disturbance fields during the hours following commencement. Most of the significant surface variations occurring during the next two days coincide with large decreases in the tail field magnitude. These variations are similar to those seen previously when electron fluxes were observed near the neutral sheet.

In Figure 25 the spacecraft is seen to traverse the neutral sheet rather quickly and to remain above it for about 12 hours. Although $\phi$ is very steady and $\theta$ is fairly steady except for about two hours, $\overline{F}$ is seen to fluctuate rapidly and widely. One may be detecting indirectly considerable particle activity just

above the neutral sheet. Once again the surface field shows large excursions coincident with the period of the greatest disturbance of $\overline{F}$.

The angle $\phi$ is seen to return to approximately 180° for the period of about six hours before the end of this run of data. This suggests that the spacecraft passes back through the neutral sheet again. A study of the position of the satellite at this time in solar magnetospheric coordinates as well as the tilting motion of the $X_{sm}$ - $Y_{sm}$ plane shows that for this to happen the neutral sheet must lie about 3 $R_E$ above the $X_{sm}$ - $Y_{sm}$ plane. A previous investigation (Ness, 1965b) revealed that there is a departure of the neutral sheet from being within a few degrees of the solar magnetospheric equatorial plane for higher geomagnetic latitudes of the sub-solar point. The encounters with the sheet by the spacecraft during this and the previous storm were seen to occur at increasingly greater distance from the $X_{sm}$ - $Y_{sm}$ plane at times only a few hours apart. In the first case the satellite was several earth radii nearer the noon-midnight meridian plane, thus suggesting that the neutral sheet may have had a negative curvature with respect to the solar magnetospheric equatorial plane during the period of these storms.

The last in the series of recurrent disturbances that have been studied in detail here occurred on May 23 at 2229 UT. Unfortunately the satellite was at perigee at that time as shown in figure 26 but the data obtained following the return of the spacecraft to the tail indicates that the tail field magnitude was indeed enhanced once again during the main phase as shown in Figure 27.

H-component decreases at 1000 UT and 1300 UT at College (Figure 13) are seen to correlate with variations in $\overline{F}$. Modulation of $\overline{F}$ by the distance of the

spacecraft from the neutral sheet is observed again, with depressed field magnitude and variable $\theta$ and $\phi$ between 2300 UT on May 24 and 0500 UT on May 25. Following this $\overline{F}$ rises to an enhanced level. Then at approximately 0900 UT there is a 10 gamma decrease in $\overline{F}$ that is accompanied by activity at all latitudes on the earth. Kakioka and Guam in the evening have trends that correlate with $\overline{F}$, while San Juan at the sunrise terminator anticorrelates. Fredricksburg and Tucson at 0200 LT and at 0400 LT, respectively, have spikes that anticorrelate with each other and occur just prior to the decrease in $\overline{F}$. The spacecraft is seen to encounter the neutral sheet again at 2200 UT on May 25 just after passage through apogee.

In this section the most significant magnetic tail and surface field variations that occurred during the 81-day period of tail field data have been described. Most of the discussion has been devoted to identifying the spatial variations in an effort to recognize purely temporal variations of consequence whenever possible. Various mechanisms for production of these time variations will be considered in the following section.

## DISCUSSION

Numerous theories have been brought forth to account for the coupling between the interplanetary medium and the magnetosphere that permits an enhanced solar wind and interplanetary magnetic field to produce observed terrestrial magnetic storm phenomena. There is general agreement that the impulse due to the impact on the magnetospheric boundary of the shock wave preceding an enhanced plasma stream is transmitted throughout the magnetosphere by hydromagnetic waves (Francis et al., 1959; Gerard, 1959; Wilson and Sugiura, 1961). The transmission of sudden impulses through the magnetosphere at close to the hydromagnetic wave speed was observed by Explorer 12 (Nishida and Cahill, 1964). Explorer 10 (Heppner et al., 1963) saw impulses that were also observed on the ground, and as was pointed out previously in this paper, the SC of the May 10, 1964 geomagnetic storm was observed at both high and low latitudes on the Earth's surface as well as deep in the magnetic tail by IMP 1. This suggests that the SC was the result of a large-scale sudden compression of the magnetosphere.

Much consideration has also been given to the possibility that there could be a "viscous" or "frictional" interaction between the solar plasma with its frozen-in magnetic field and the field lines and materials of the outer magnetosphere (Parker, 1958; Piddington, 1959, 1960; Axford and Hines, 1961; Dessler and Walters, 1964). The general conclusion has been that instabilities at the boundary would leads to an effective viscosity, and the momentum transfer process and "scattering" of the geomagnetic field at the boundary would lead to a sweeping up of field and boundary material by the solar plasma. Axford and

Hines based their theoretical picture of a magnetospheric convection pattern that could drive ionospheric current systems on this continuous transport of ionized material to the tail. There it would finally be constrained and would flow back toward the Earth in the interior of the tail.

Dungey (1961, 1963) discussed the possibility of connection taking place between interplanetary and geomagnetic field lines at neutral points if the interplanetary field had a southward component. Such a model has been considered in more detail by Levy et al. (1964). They suggest that if the interplanetary magnetic field is generally southward then there should be a connecting of interplanetary field lines with magnetospheric lines at the subsolar point. As the solar wind sweeps past the Earth these lines would then be swept across the poles and into the tail, where they would ultimately become disconnected again. Magnetospheric lines that have become reconnected would then return to the front of the magnetosphere, flowing around the sides in low latitudes. For a steady state condition the rate at which field lines become joined must equal the rate at which they become detached.

Taking the view that ionospheric currents could be due mainly to the motion of electrons frozen to the field lines, which are free to slide over the top of the ionosphere, then the polar current system would be produced by the flowing of field lines across the polar regions in the antisolar direction and returning in a lower latitude band. As long as some joining of field lines occurs, the lines will be dragged in a generally antisolar direction. Levy et al. estimate that approximately 1/5 of the interplanetary lines will become connected to magnetospheric lines under normal conditions. This is in good agreement with the

observed flow rates in the ionosphere and is sufficient to drive an interval convection pattern.

Magnetic measurements in interplanetary space lend some support to this model. Pioneer V measured a steady component of the interplanetary field normal to the ecliptic plane (Coleman et al, 1960). IMP 1 found that the interplanetary field vector tended to lie near the ecliptic plane but had a southward component of 0.5 - 1.0 gammas during 2/3 of the 3-hour intervals of interplanetary observations (Ness and Wilcox, 1964).

A comparison of Explorer 12 measurements of the magnetic field outside the magnetosphere with magnetograms from arctic observatories (Fairfield and Cahill, 1965) has suggested that an exterior field with a southerly component tends to be associated with a ground disturbance while a northward field is associated with quiet conditions. They point out that while the field reconnection model appears to explain the observed results in general, it fails to account for the onset of large bay events or polar substorms. The dramatic suddenness with which bay events often begin suggests that some kind of instability is involved.

Axford et al. (1965) have discussed the manner in which magnetic field lines that have been swept into the tail are annihilated, thereby converting magnetic energy into plasma energy at the neutral sheet. Piddington (1965) has computed that the heating of the plasma by the energy released in this manner provides approximately 4000 eV per particle if the particle density is 1 $cm^{-1}$ and the tail field magnitude is 40 gammas. Some of this energy is thermal and

some kinetic energy of mass motion. He suggests that field lines thus travel as hydromagnetic waves until they return to the approximately dipolar region of the magnetosphere and are absorbed at a magnetic latitude of about 68°. He further suggests that in returning to the front of the magnetosphere to replace those lines being dragged to the tail, field lines cannot flow forward around the boundary because of the friction that they would encounter there. Hence the return path should be within the magnetosphere, on a shell of constant geomagnetic latitude.

Taylor and Hones (1965) point out that although proponents of the field line reconnection theory cite as support for their theory the fact that the polar cap ionospheric current system is aligned toward the Sun, several analyses of polar region field variations (Silsbee and Vestine, 1942; Sugiura and Chapman, 1960) have led to the belief that the system is more often directed between 60° and 90° west of the Sun. A more recent study of the magnetograms from 25 high-northern-latitude observatories by Fairfield (1963) has led to the conclusion that in quiet times the current system is most often oriented 65° west of the Sun. During disturbed times, however, it shifts to approximately 30° west of the Sun, and the time variations are large in both intensity and direction.

The angles 30° and 65° west of the Sun correspond to the theoretical streaming angles that the interplanetary magnetic field would have due to solar wind velocities of 200 and 750 km/sec, respectively. Thus there is a possibility that the direction taken by field lines being swept across the poles following reconnection will be controlled by the streaming angle of the interplanetary part of the line. This direction would then vary with the degree of enhancement

of the solar wind. Because the geomagnetic end of a line remains attached at the Earth, the line becomes stretched out in the antisolar direction when it becomes a part of the tail.

To account for the increases seen in tail field magnitude during geomagnetic storms utilizing field reconnection requires that there be an accumulation of field lines in the tail. This would mean that during times of high solar plasma velocity lines would be swept into the tail faster than they could be replaced from within, increasing the tail field magnitude and at the same time, with some time lag, depressing the low latitude dipole field. Akasofu and Chapman (1963a, b) and Akasofu (1964) have pointed out, however, that an enhancement of the solar wind flow is not always followed by development of a geomagnetic storm main phase. They propose that there must be some additional property associated with the solar plasma flow. As Fairfield and Cahill (1965) have suggested, the directional characteristics of the interplanetary field may be important in the production of a sufficiently non-steady state condition for the substantial accumulation of magnetic flux in the tail.

Although he allows that bringing in new field lines may account for a part of the observed increase in magnetic flux in the tail during times of disturbance, Cahill (1965) suggests that the fluctuations in tail field direction and the increase in magnitude may be the result of compression by the enhanced solar plasma. He estimates that during one storm observed by Explorer 14 the tail was compressed to 2/3 to 1/2 of its normal radius if the increase in field magnitude was due only to the compression of lines already in the tail.

It is difficult to see how one could determine whether the increase in tail field magnitude is produced by the addition of new field lines or the compression of existing lines unless a spacecraft was situated so as to be able to measure the distance that the tail boundary moves in under compression. Such motion of the boundary was detected by Explorer 10 (Heppner et al., 1963). Both effects can quite reasonably be expected to accompany an enhanced solar plasma, although the additional requirement concerning a southward interplanetary field component would not apply to the compression case.

The April 1, 1964 storm observed on IMP-I during orbit No. 33 provided an ideal opportunity to separate the two possible effects. Wolfe (private communication) has reported that no plasma flux was observed by the electrostatic analyzer during orbits 31-48 of IMP-I except for a very short period on April 1 from approximately 2100 to 2400 UT. This observation is interpreted as representing the movement of the magnetosphere boundary past the satellite towards the Earth-Sun line so that IMP-I was immersed with the magnetosheath for this brief interval. This one observation is fortuitous for on orbit 33 the plasma was detected shortly after the satellite passed through apogee.

It is possible to show that additional lines of force from the geomagnetic field were extended into the tail during this event. For this study it will be assumed that the colatitude of the polar cap region ($\theta_{pc}$) to which lines of force from the tail connect is related to the radius ($R_T$) of the tail and field strength ($B_T$) as

$$B_T = 4 B_0 \left(\frac{R_E}{R_T}\right)^2 \sin^2 \theta_{pc}$$

where $B_o$ is the equatorial field strength (Ness, 1965b). The distance of the satellite from the Earth-Sun line is measured by

$$D_{xy} = \sqrt{Y_{sm}^2 + Z_{sm}^2} = \sqrt{RAD^2 - X_{sm}^2} = \sqrt{RAD^2 - X_{se}^2}$$

Since the satellite was close to apogee when the storm occurred, the value of $D_{xy}$ for the time interval under consideration was approximately constant and equal to 16.8 $R_E$. How far beyond this the magnetosphere boundary was located on March 31 was not directly measured. Earlier data from IMP-1 (Ness, 1965b) suggest the value of $R_T$ during quiet times as approximately 20-22 $R_E$.

The field is observed (see figures 15 and 16) to be approximately 15 gammas preceding the storm and hence $\theta_{pc}$ = 13 - 14°. Shortly before the storm at 1525 and for 5 hours after, but before plasma was observed, the field strength is increased to approximately 35-40 gammas. Assuming that the boundary moves in to just slightly greater than $D_{xy}$ = 16.8 $R_E$ before the plasma is observed yields an estimate of $\theta_{pc}$ = 16° - 17°.

Thus, in this elementary interpretation, it appears that additional lines of force, originating in the polar cap at $\theta_{pc} \doteq$ 14° - 16°, are dragged into the tail by the increased plasma flux from the Sun. It should be noted that approximately 50% of the field increase can be attributed to simple compression of the tail. Further studies on this complex phenomenon will be required to delineate more precisely and with better statistics the relative roles played by these two mechanisms. It appears certain from these IMP-I data that both are important in geomagnetic storm phenomenon in the Earth's tail.

As discussed briefly in the introduction, there is considerable experimental evidence of particle activity outside the stable trapping region on the dark side of the Earth. Gringauz et al. (1960) and Freeman (1964) have found large fluxes of low energy electrons just outside the stable trapping region. Frank (1965) has found evidence of the existence of an "electron tail" of the magnetosphere. Singer et al. (1965) have observed enhanced fluxes of $E > 40$ keV electrons in the vicinity of the neutral sheet region.

Observing electrons with $E > 50$ keV at 17.7 $R_E$ with the Vela satellites, Montgomery et al. (1965) found a clustering of events about the geomagnetic equatorial plane and rapid time variations in flux that appear to be evidence of particle acceleration. Asbridge et al. (1965) have also reported on the Vela experiments and have stated that numerous examples of electrons flowing outward from the general direction of the Earth have been observed. The flow duration was from minutes to hours. On one day for two periods of eight minutes separated by three hours, 5 keV protons were observed streaming toward the Earth.

Studies of the luminescence of the moon have revealed the fact that the moon has been close to full in all instances of intense luminescence. Thus it may have been exposed to beams of accelerated particles in the magnetic tail (Cameron, 1964). The clustering of electron fluxes near the antisolar direction and the observation of accelerated beams of electrons by IMP 1 near the neutral sheet (Anderson, 1965a; Anderson et al., 1965) suggest that the neutral sheet is the site of the acceleration mechanism.

Piddington (1965) has predicted hydromagnetic waves traveling in the neutral sheet. The possibility that hydromagnetic waves might produce particle acceleration has been discussed by Thompson (1955) and Parker (1955) in connection with cosmic rays and by Dessler (1958) in connection with energetic magnetospheric particles. It may be that enhanced wave activity during disturbances could produce the observed acceleration.

Cahill (1965) has suggested that the compression of the neutral sheet might provide a mechanism for accelerating particles and producing their precipitation along lines of force into the auroral zones. He further suggests that the pocket of hot plasma outside the stable trapping region on the night side may also be a source region for auroral particles. The location of this pocket of plasma at the near-Earth end of the neutral sheet might subject it to the effects of compression of wave propagation from the tail. McDiarmid and Burrows (1965) interpret the high latitude electron spikes observed at 1000 km by the Alouette 1 satellite to be related to the "electron islands" observed by Anderson et al. (1965). They point out that since some of the intensities in the electron spikes are as much as three orders of magnitude higher than those reported by Anderson et al, this may indicate acceleration mechanisms are acting on the particles as they travel from in or near the neutral sheet to the vicinity of the Earth. They further suggest that electrons generated in the tail may form an important source of electrons for the outer radiation zone.

From Injun 3 satellite measurements O'Brien and Taylor (1963) have concluded that auroras occur at the high-latitude boundary of electron trapping and that they probably delineate this boundary. They state that it is uncertain

whether the auroral acceleration mechanism occurs on the last closed lines of force or the first open ones or straddling them, but do conclude that the electrons seen were freshly accelerated. McIlwain (1960) had previously directly observed particles producing visible auroras and had found that they were nearly monoenergetic electrons with about 6 keV energy. On the basis of this he suggested an electrostatic acceleration mechanism for the particles.

In a model of the magnetosphere which includes the effects of solar wind pressure on the sunward side, a current sheet in the tail and magnetic field lines in the tail which are equipotentials, Taylor and Hones (1965) propose that auroral events are produced largely by electrostatic acceleration of solar wind electrons which enter on the evening side of the tail and are subsequently energized by the electric fields. In contrast, Dessler and Juday (1965) have proposed that the auroral radiation is energized at the magnetopause along the tail where the solar and magnetospheric plasmas are in relative motion. McDiarmid and Burrows (1965) point out that this model would require a uniform distribution in local time of high latitude electron spikes and this is not in agreement with observation.

It appears then that there is quite a substantial body of theoretical and experimental support for the acceleration of auroral particles in or near the neutral sheet. The exact acceleration mechanism is not known, but it seems to be intimately connected to the increase of magnetic flux density in the tail. Considering the suddenness of some magnetic field decreases observed in the tail by IMP 1 and the similar sudden appearance of electron beams, some instability process such as a sheet pinch instability (Furth et al., 1963) may be a part of the acceleration mechanism, as suggested by Ness (1965b).

Since it seems likely that the tail is capable of capturing particles from the solar wind and is capable of accelerating these particles, then the tail is the most likely source of a "ring current" at times of enhanced solar plasma flux and pressure. A diamagnetic ring current encircling the earth during the main phase of a geomagnetic storm has long been invoked to account for the low latitude decrease observed in the horizontal component. The significant differences in modern ring current theories (Singer, 1957; Dessler and Parker, 1959; Dessler et al, 1961; Akasofu and Chapman, 1961) lie in the mechanisms for getting the particles into the geomagnetic cavity and energizing them there. Most all of them suggest that the current lies at a distance of 5 to 8 $R_E$.

Vanguard 3 (Cain et al, 1962) demonstrated that the source of the main field depression at low latitudes must be at altitudes greater than that of maximum radiation intensity in the inner radiation belt. The measurements of Explorer 10 (Heppner et al, 1963) were not inconsistent with a ring current below the magnetic shell intersecting the equator at 3.8 $R_E$. Also Electron II data (Dolginov et al., 1966) were suggestive of the existence of a ring current during geomagnetic disturbances. Explorer VI (Smith et al., 1964) yielded inconclusive results on a permanent ring current on final analysis.

Thus, although the ring current responsible for the main phase decrease has not been positively verified experimentally, there is still a possibility that it is a physical reality. If the tail is the source of ring current particles produced by some mechanism related to the increase in magnetic flux density, then this could account for the fact that during the April 1 and May 10 storms the main phase began after the magnetic flux density in the tail reached a sustained high level.

Hoffman and Bracken (1965) postulate that the storm-time ring current is due to protons in the 1 to 100 keV range. Protons are chosen because trapped electrons observed to date produce negligible magnetic fields. They further point out that there must be a source and probably an acceleration mechanism for replenishing the population. One hesitates to suggest that the magnetic tail supplies the ring current with protons when there is almost no evidence to date of protons streaming in the tail, although the model of Taylor and Hones (1965) includes the capture of solar wind protons by the tail to provide the particles that are precipitated in auroral regions.

Two of the geomagnetic disturbances considered in detail in this investigation began without any sudden commencement or initial phase field increase at low latitudes. There were further characterized by highly irregular field variations. Akasofu (1965) has considered the class of $S_g$ (gradually commencing) storms and has concluded that such storms can develop without significant enhancement of the solar plasma pressure. He proposes that such storms are produced by solar plasma streams consisting mainly of neutral hydrogen atoms. These atoms penetrate deep into the magnetosphere and become ionized by collision with atmospheric particles. These ionized particles could then contribute to the production of a significant ring current.

As was discussed previously, Wilcox and Ness (1965) have shown that the portion of interplanetary sectors which produces geomagnetic activity is a region of enhanced plasma flow. It may be that at times there is a more gradual increase of the solar wind flux, so that mechanisms producing the low latitude decrease take effect before the plasma can produce any detectable compression of the dipole part of the field. Also, it is difficult to see how the

neutral hydrogen atom mechanism could produce the tail field magnitude variations that anticorrelate so well with the low latitude storm field variations.

Attempts to identify the various mechanisms producing geomagnetic disturbances have in recent years included statistical examinations of possible variation of geomagnetic activity with lunar phase. Bigg (1963a, b) reported finding a decrease of geomagnetic activity at new moon. Davidson and Martyn (1964) and Michel et al. (1964) were, however, unable to find any dependence of terrestrial magnetic activity on lunar phase. Meanwhile both Bell and Defouw (1964) and Stolov and Cameron (1964) independently reported finding a decrease of geomagnetic disturbance for several days before full moon and an increase for several days after full moon during the last 31 years. Both the decrease and the increase amounted to approximately 4%. Shapiro and Ward (1965) found a 29.5-day peak in addition to the 27-day peak in the power spectrum of Kp.

Stolov (1965) claims greater statistical significance for the analyses that found a full moon effect. He also has found that there is evidence that the observed variation of geomagnetic activity with lunar phase requires lunar latitudes at full moon within about 4° from the ecliptic plane. This is a distance of approximately 4 $R_E$. There is no evidence for a lunar effect on geomagnetic activity during disturbed periods (Stolov and Cameron, 1964).

The sort of interaction that one should expect between the moon and the Earth's magnetic tail is not completely clear. A disturbance due to the moon was detected in the interplanetary medium by the IMP 1 satellite (Ness, 1965a)

but this was simply the magnetohydrodynamic wake caused by the moon being a solid, spherical obstruction in the solar plasma flow.

Previous attempts to measure a lunar magnetic field (Dolginov et al., 1961) have indicated that if such a field exists it must be less than 50-100 gammas at the surface.

Thus the possible types of interaction seen to be limited to some sort of disturbance of the plasma in the tail. The finding of a necessity for the passage to be near the ecliptic plane suggests the possibility of an interaction with the neutral sheet. It is difficult to see how such an interaction could have the asymmetric properties with respect to the noon-midnight meridian plane that were found statistically when the effect is averaged over many full moons.

Attempts to detect any geomagnetic effects produced by the moon's passage through the Earth's magnetic tail during the period that IMP 1 was mapping the tail are complicated by the fact that the successive occurrences of full moon during the period of tail data were near times of geomagnetic storms. Figure 28 shows the relative positions of the moon and the IMP 1 spacecraft during three successive passes of the moon through the tail as viewed from the Earth. Ecliptic coordinates are used with the distance units again being Earth radii. The shaded areas are the regions of the tail swept out by the daily oscillation of the solar magnetospheric equatorial plane about the $-X_{sm}$ axis during the days considered.

## CONCLUSIONS

From the observational evidence presented and the discussion of its various details and pertinent theoretical models, it appears that the correlated temporal variations of the magnetic field in the tail and on the earth's surface can be generally classified into two characteristic types:

1. Positive correlations, in which increases in the magnitude of both the tail field and H-component of the geomagnetic field occur and
2. Negative correlations, for which an increase in tail field magnitude and planetary index Kp is accompanied by a decrease in the H-component of the terrestrial field.

Although this separation of tail field phenomenon into only two categories is elementary, the observational data tend to support these conclusions rather directly. A difficult task in the analysis of the large quantity of data has been the identification of those spatial variations associated with the changing relative position of the neutral sheet and the satellite as well as temporal variations associated with transient electron fluxes altering the local magnetic field.

As originally discussed by Parker (1958) these two classes of correlated behavior can be viewed in terms of a physical pressure or tension of the geomagnetic field respectively. The pressure is due to the interaction of the enhanced solar wind on the geomagnetic field, particularly on the sunlit hemisphere portion of the magnetosphere. The tension is due to the permanent existence of the geomagnetic tail (Ness, 1965b) and its observed variable strength leading to variable tension on the geomagnetic field. The most striking example of the two

classes of correlation occur in the magnetic storm studied on May 10th, the sudden commencement occurring at 0035 UT. Subsequently the main phase of the storm develops and displays the anticorrelation of tail field magnitude and terrestrial field which was anticipated by Axford et. al. (1965).

This general behavior during the main phase is observable in the other storms studied. The effect of an increased tail field magnitude at the time of the main phase has also been studied from another point of view by Ness and Williams (1966). Invoking a tail field model of the geomagnetic field these authors have demonstrated the positive correlation between an increased tail field magnitude and lowered trapping boundary on the night side of the earth. This is to be expected from the anticorrelation of tail field magnitudes and H-component of the terrestrial field. The planetary magnetic index Kp is observed to be positively correlated with tail field magnitude. As originally obtained from the work on Mariner II by Snyder, Neugebauer and Rao (1963) Kp is an effective index of the solar wind velocity.

A unique opportunity to investigate the relative contributions of compression of the tail and the addition of new lines of force to the increased tail field strength occurred during orbit No. 33. It is concluded that in response to an enhanced solar plasma flow a substantial number of additional lines of force are extended from the geomagnetosphere into the earth's magnetic tail. This is a most important conclusion of this study of correlated terrestrial data with satellite data.

Piddington (1960) suggested a tail field topology similar to that observed by IMP-I to explain the phenomenon of the geomagnetic storm. However in his model

the geomagnetic tail was not a permanent feature of the distorted magnetosphere. Axford et. al. (1965), Dessler (1964), and Dessler and Juday (1965) have considered a geomagnetic tail as a permanent feature of the solar wind interaction with the geomagnetic field. Axford et. al. (1965) has further suggested that magnitude changes in the magnetic tail field should be approximately equal to but anticorrelated with the geomagnetic H-component. Although anticorrelation is observed, equality is not observed, since the tail field rises from 10 to 20 gammas to approximately 20 to 40 gammas during the magnetic storms studied during this particular period of time. Such a magnitude rise is insufficient to explain the terrestrial observations so that a non-linear or more complex relationship between tail field and terrestrial field disturbance must be postulated. Also evident in the data is the existence of a small component of field traverse to the neutral sheet at the time of traversals which are consistent with a merging of field lines across the neutral sheet, as suggested by Axford et. al. (1965). Thus Figure 2 of this paper indicating no connection across the neutral sheet is not truly representative of the field component normal to the sheet.

The problem of the interaction of the Moon with the geomagnetic tail is not clarified by these studies. During three successive passes of the moon thru the tail region, corresponding to full moon, no distinctive and identifiable changes were observable in the tail field data. These phenomenon were somewhat obscured by the magnetic storms observed coincident with the passage of the moon through the tail, however.

Various theories have been proposed to explain the 27 day recurrent geomagnetic activity phenomenon known as M-region magnetic storms. Certain

authors have suggested distinctive differences in the emission of plasma from the sun to explain these observations. From the data observed by IMP-I and the studies by Wilcox and Ness (1965) it appears that this particular class of magnetic activity is more directly related to variations in the corotating structure of the plasma flow within the interplanetary medium. Thus, this supports the initial suggestions by Dessler and Fejer (1963) that M-region storms are a phenomenon to be associated more directly with a corotating structure in the interplanetary medium rather than with specific characteristics identifiable on the surface of the sun.

ACKNOWLEDGMENTS

We are indebted to our co-workers Mr. C. S. Scearce and Mr. J. B. Seek for their important participation in the experimental work reported upon here. We also appreciate the discussions of these results and their significance with Drs. M. Sugiura, J. M. Wilcox, and D. J. Williams. We appreciate the opportunity to employ the plasma results of Dr. J. Wolfe in advance of publication.

REFERENCES

Akasofu, S.-I., The development of geomagnetic storms after a negative sudden impulse, Planet. Space Sci., 12, 573-578, 1964.

Akasofu, S.-I., The development of geomagnetic storms without a preceding enhancement of the solar plasma pressure, Planet. Space Sci., 13, 297-301, 1965.

Akasofu, S.-I. and S. Chapman, The ring current, geomagnetic disturbance and the Van Allen radiation belts, J. Geophys. Res., 66, 1321-1350, 1961.

Akasofu, S.-I. and S. Chapman, The development of the main phase of magnetic storms, J. Geophys. Res., 68, 125-129, 1963a.

Akasofu, S.-I. and S. Chapman, Magnetic storms: the simultaneous development of the main phase (DR) and of polar magnetic substorms (DP), J. Geophys. Res., 68, 3155-3158, 1963b.

Allen, C. W., Relation between magnetic storms and solar activity, Mon. Not. Roy. Ast. Soc., 104, 13-21, 1944.

Allen, C. W., M-regions, Planet. Space Sci., 12, 487-494, 1964.

Anderson, K. A., Energetic Electron Fluxes in the Tail of the Geomagnetic Field, J. Geophys. Res. 70, 4741-4763, 1965a.

Anderson, K. A., Radial dependence of energetic electron fluxes in the tail of the Earth's magnetic field, Phys. Rev. Letters, 14, 888-890, 1965b.

Anderson, K. A., H. K. Harris and R. J. Paoli, Energetic electron fluxes in and beyond the Earth's outer magnetosphere, J. Geophys. Res., 70, 1039-1050, 1965.

Asbridge, J. R., S. J. Bame, H. E. Felthauser, R. A. Olson and I. B. Strong, Streaming of electrons and protons in the Earth's magnetospheric tail at 17 Earth radii, Presented at 46th Annual Meeting of the A.G.U., Washington D. C., April 19-22, 1965.

Axford, W. I., Viscous interaction between the solar wind and the Earth's magnetosphere, Planet. Space Sci., 12, 45-53, 1964.

Axford, W. I. and C. O. Hines, A unifying theory of high-latitude geophysical phenomena and geomagnetic storms, Can. J. Phys., 39, 1433-1464, 1961.

Axford, W. I., H. E. Petschek, and G. L. Siscoe, The tail of the magnetosphere, J. Geophys. Res., 70, 1231-1236, 1965.

Bartels, J., Terrestrial-magnetic activity and its relations to solar phenomena, Terr. Magnetism and Atmos. Elec., 37, 1-52, 1932.

Behannon, K. W. and N. F. Ness, The design of numerical filters for geomagnetic data analysis, to appear as a NASA Tech. Note, 1965.

Bell, B., Major flares and geomagnetic activity, Smithson. Contrib. to Astrophys., 5, 69-83, 1961.

Bell, B. and R. J. Defouw, Concerning a lunar modulation of geomagnetic activity, J. Geophys. Res., 69, 3169-3174, 1964.

Bigg, E. K., The influence of the moon on geomagnetic disturbances, J. Geophys. Res., 68, 1409-1413, 1963a.

Bigg, E. K. Lunar and planetary influences on geomagnetic activity, J. Geophys. Res., 68, 4099-4104, 1963b.

Boulder High Altitude Observatory, Boulder, Colorado; Preliminary reports of solar activity, TR 655-666, March-June, 1964.

Bridge, H., A. Egidi, A. Lazarus, E. Lyon and L. Jacobson, Preliminary results of plasma measurements on IMP-A, Space Research V, 969-978, North-Holland Publishing Co., Amsterdam, 1965.

Bumba, V. and R. Howard, Large-scale distribution of solar magnetic fields, Ap. J., 141, 1502-1512, 1965.

Cahill, L. J., Jr., Inflation of the magnetosphere near 8 Earth radii in the dark hemisphere, Univ. of New Hampshire Dept. of Phys. pub. UNH 65-4, Durham, New Hampshire, 1965.

Cain, J. C., I. R. Shapiro, J. D. Stolarik, and J. P. Heppner, Vanguard 3 magnetic-field observations, J. Geophys. Res., 67, 5055-5069, 1962.

Cameron, A. G. W., Particle Acceleration in Cislunar Space, Nature, 202, 785, 1964.

Central Radio Propagation Laboratory, Boulder, Colorado; Part B-Compilation of Solar-Geophysical Data, CRPL-F 236-239, April-July 1964.

Coleman, P. J., Jr., L. Davis and C. P. Sonett, Steady component of the interplanetary magnetic field: Pioneer V, Phys Rev. Letters, 5, 43-48, 1960.

Davidson, T. W. and D. F. Martyn, A supposed dependence of geomagnetic storminess on lunar phase, J. Geophys. Res., 69, 3973-3979, 1964.

Dessler, A. J., Large amplitude hydromagnetic waves above the ionosphere, J. Geophys. Res., 63, 507-511, 1958.

Dessler, A. J. and J. A. Fejer, Interpretation of Kp index and M-region geomagnetic storms, Planet. Space Sci., 11, 505-511, 1963.

Dessler, A. J., W. B. Hanson and E. N. Parker, Formation of the geomagnetic main phase ring current, J. Geophys. Res., 66, 3631-3637, 1961.

Dessler, A. J. and R. D. Juday, Configuration of auroral radiation in space, Planet. Space Sci., 13, 63-72, 1965.

Dessler, A. J. and E. N. Parker, Hydromagnetic theory of geomagnetic storms, J. Geophys. Res., 64, 2239-2252, 1959.

Dessler, A. J. and G. K. Walters, Hydromagnetic coupling between the solar wind and the magnetosphere, Planet. Space Sci., 12, 227-234, 1964.

Dolginov, S. H., E. G. Eroshenko, L. N. Zhugov, N. V. Pushkov and L. O. Tynrmina, Investigation of the magnetic field of the moon, Geomagnetizm Aeronomiya, 1, 21-29, 1961.

Dolginov, Sh. Sh., Ye. G. Yeroshenko and L. N. Zhuzgov, A Survey of the Earth's Magnetosphere in the Region of the Radiation Belt (3-6 $R_e$) from February to April 1964, Space Research VI, to appear, 1966.

Dungey, J. W., Interplanetary magnetic field and the auroral zones, Phys. Rev. Letters, 6, 47-48, 1961.

Dungey, J. W., Structure of the exosphere or adventures in velocity space, Geophysics the Earth's Environment, 505-550, Gordon and Breach, New York, 1963.

Fairfield, D. H., Ionospheric current patterns in high latitudes, J. Geophys. Res., 68, 3589-3602, 1963.

Fairfield, D. H. and L. J. Cahill, Jr., The interplanetary magnetic field and polar magnetic disturbances, Univ. of New Hampshire Dept. of Physics pub. UNH-65-1, Durham, New Hampshire, 1965.

Fejer, J. A., Geometry of the Magnetospheric Tail and Auroral Current Systems, J. Geophys. Res. 70, 4972-4975, 1965.

Finch, H. F. and B. R. Leaton, The Earth's main magnetic field-epoch 1955, Mon. Not. Roy Ast. Soc., 4, 314-317, 1957.

Francis, W. E., M. I. Green and A. J. Dessler, Hydromagnetic propagation of sudden commencements of magnetic storms, J. Geophys. Res., 64, 1643-1645, 1959.

Frank, L. A., A survey of electrons beyond 5 $R_E$ with Explorer XIV, J. Geophys. Res., 70, 1593-1626, 1965.

Freeman, J. W., Electron distribution in the outer radiation zone, J. Geophys. Res., 69, 1691-1724, 1964.

Furth, H. P., J. Killeen and M. N. Rosenbluth, Finite-resistivity instabilities of a sheet pinch, Phys. of Fluids, 6, 459-484, 1963.

Gerard, V. B., The propagation of world-wide sudden commencements of magnetic storms, J. Geophys. Res., 64, 593-596, 1959.

Gringauz, K. I., Some results of experiments in interplanetary space by means of charged particle traps on soviet space probes, Space Research II, 539-553, North Holland Publishing Co., Amsterdam, 1961.

Gringauz, K. I., V. G. Kurt, V. I. Moroz, and I. S. Shklovsky, Results of observations of charged particles observed out to 100,000 km with the aid of charged particle traps on Soviet space probes, Astron. Zh., 37-4, 716-735, 1960.

Heppner, J. P., N. F. Ness, C. S. Scearce and T. L. Skillman, Explorer 10 magnetic field measurements, J. Geophys. Res., 68, 1-46, 1963.

Hoffman, R. A. and P. A. Bracken, Magnetic effects of the quiet-time proton belt, J. Geophys. Res., 70, 3541-3556, 1965.

Jenkins, R. W. and I. Paghis, Criterion for the association of solar flares with geomagnetic disturbances, Can. J. Phys., 41, 1056-1075, 1963.

Levy, R. H., H. E. Petschek and G. L. Siscoe, Aerodynamic aspects of the magnetospheric flow, AIAA Journal 2, 2065-2096, 1964.

Lincoln, J. V., Geomagnetic and solar data, J. Geophys. Res., 70, 1227, 1965a.

Lincoln, J. V., Geomagnetic and solar data, J. Geophys. Res., 70, 2233, 1965b.

McDiarmid, I. B. and J. R. Burrows, Electron fluxes at 1000 kilometers associated with the tail of the magnetosphere, J. Geophys. Res., 70, 3031-3044, 1965.

McIlwain, C. E., Direct measurement of particles producing visible auroras, J. Geophys. Res., 65, 2727-2747, 1960.

Montgomery, M. D., S. Singer, J. P. Conner, and E. E. Stogsdill, Spatial distribution, energy spectra and time variations of energetic electrons (E > 50 keV) at 17.7 earth radii, Phys. Rev. Letters, 14, 209-213, 1965.

Michel, F. C., A. J. Dessler and G. K. Walters, A search for correlation between Kp and the lunar phase, J. Geophys. Res., 69, 4177-4183, 1964.

Mustel, E., Quasi-stationary emission of gases from the Sun, Space Science Revs., 3, 139-231, 1964.

Ness, N. F., The magnetohydrodynamic wake of the moon, J. Geophys. Res., 70, 517-534, 1965a.

Ness, N. F., The Earth's magnetic tail, J. Geophys. Res., 70, 2989-3005, 1965b.

Ness, N. F., C. S. Scearce and J. B. Seek, Initial results of the IMP 1 magnetic field experiment, J. Geophys. Res., 69, 3531-3570, 1964.

Ness, N. F., C. S. Scearce, J. B. Seek and J. M. Wilcox, A summary of results from the IMP 1 magnetic field experiment, submitted to Space Research VI, 1965.

Ness, N. F. and J. M. Wilcox, The solar origin of the interplanetary magnetic field, Phys. Rev. Letters, 13, 461-464, 1964.

Ness, N. F., and J. M. Wilcox, Sector Structure of the Quiet Interplanetary Magnetic Field, Science, 148, 1592-1594, 1965.

Ness, N. F. and J. M. Wilcox, Extension of the Photospheric Magnetic Field into Interplanetary Space, Ap. J., to appear, 1966.

Ness, N. F. and D. J. Williams, Correlated Magnetic Tail and Radiation Belt Observations, J. Geophys. Res. 71(1), 1966.

Newton, H. W., Solar flares and magnetic storms, Mon. Not. Roy. Ast. Soc., 104, 4-12, 1944.

Nishida, A. and L. J. Cahill, Sudden impulses in the magnetosphere observed by Explorer 12, J. Geophys. Res., 69, 2243-2255, 1964.

O'Brien, B. J. and H. Taylor, High latitude geophysical studies with satellite Injun 3, 4. Auroras and their excitation; J. Geophys. Res., 69, 45-63, 1964.

Parker, E. N., Hydromagnetic waves and the acceleration of cosmic rays, Phys. Rev., 99, 241-253, 1955.

Parker, E. N., Interaction of the solar wind with the geomagnetic field, Phys. Fluids, 1, 171-187, 1958.

Pecker, J. C. and W. O. Roberts, Solar corpuscles responsible for geomagnetic disturbances, J. Geophys. Res., 60, 33-44, 1955.

Piddington, J. H., The Transmission of Geomagnetic Disturbances through the atmosphere and interplanetary Space, Geophys. J., 2, 173-189, 1959.

Piddington, J. H., Geomagnetic storm theory, J. Geophys. Res., 65, 93-106, 1960.

Piddington, J. H., Recurrent geomagnetic storms, solar M-regions and the solar wind, Planet. Space Sci., 12, 113-118, 1964.

Piddington, J. H., The magnetosphere and its environs, Planet. Space Sci., 13, 363-376, 1965.

Saemundssen, Th., Statistics of geomagnetic storms and solar activity, Mon. Not. Roy. Ast. Soc., 123, 299-316, 1962.

Sarabhai, V., Some Consequences of Non-Uniformity of Solar Wind Velocity, J. Geophys. Res. 68, 1555-1557, 1963.

Scherb, F., Velocity distribution of interplanetary plasma detected by Explorer 10, Space Research IV, 797-818, North Holland Publishing Co., Amsterdam, 1964.

Shapoir, R. and F. Ward, private communication, to be published, 1965.

Silsbee H. C. and E. H. Vestine, Geomagnetic bays, their frequency and current systems, Terr. Magnetism and Atmos. Elec., 47, 195-208, 1942.

Simpson, J. A., H. W. Babcock and H. D. Babcock, Association of a "unipolar" magnetic region on the Sun with changes of primary cosmic-ray intensity, Phys. Rev., 98, 1402-1406, 1955.

Singer, S., J. P. Conner, W. D. Evans, M. D. Montgomery, and E. E. Stogsdill, Plasma observations at $10^5$ km, Space Research V, 546-563, North Holland Publishing Co., Amsterdam, 1965.

Singer, S. F., A new model of Magnetic Storms and Aurorae, Trans. Am. Geophys. Union, 38, 175-190, 1957.

Smith, E. J., C. P. Sonett and J. W. Dungey, Satellite observations of the geomagnetic field during magnetic storms, J. Geophys. Res., 69, 2669-2688, 1964.

Snyder, C. W., M. Neugebauer and U. R. Rao, The solar wind velocity and its correlation with cosmic-ray variations and with solar and geomagnetic activity, J. Geophys. Res., 68, 6321-6370, 1963.

Stolov, H. L., Further investigations of a variation of geomagnetic activity with lunar phase, J. Geophys. Res., 70, 4921-4926, 1965.

Stolov, H. L., and A. G. W. Cameron, Variations of geomagnetic activity with lunar phase, J. Geophys. Res., 69, 4975-4982, 1964.

Sugiura, M. and S. Chapman, The average morphology of geomagnetic storms with sudden commencements, Abhandl. Akad, Wiss. Goettingen, Math-Physik Kl., 4, 3-53, 1960.

Taylor, H. E. and E. W. Hones, Jr., Adiabatic motion of auroral particles in a model of the electric and magnetic fields surrounding the Earth, J. Geophys. Res., 70, 3605-3628, 1965.

Thompson, W. B., On the acceleration of cosmic ray particles by magneto-hydrodynamic waves, Proc. Roy. Soc. A, 233, 402-406, 1955.

Wentworth, R. C., Diamagnetic Ring Current Theory of the Neutral Sheet and its Effects on the Topology of the anti-solar magnetosphere, Phys. Rev. letters, 14, 1008-1010, 1965.

Wilcox, J. M. and N. F. Ness, A quasi-stationary co-rotating structure in the interplanetary medium, J. Geophys. Res., 70(23), 1965.

Wilson, C. R. and M. Sugiura, Hydromagnetic interpretation of sudden commencements of magnetic storms, J. Geophys. Res., 66, 4097-4111, 1961.

LIST OF FIGURES

latitude of the subsolar point; $\theta_{sm}$ (dashed line), the solar magnetospheric latitude of the subsatellite point; and $Z_{sm}$ (dotted line), the perpendicular distance of the satellite from the solar magnetospheric equatorial plane. Vertical solid lines mark observed neutral sheet crossings.

Figure 6. Planetary 3-hourly geomagnetic activity index Kp, magnetic tail field magnitude $\overline{F}$ observed by IMP 1, and local disturbance fields at selected magnetic observatories for the period March 15 - April 10, 1964. Storm commencement times (UT) are given.

Figure 7. Planetary 3-hourly index Kp and RMS deviations of local disturbance fields at selected magnetic observatories for the period March 15 - April 10, 1964. (See Figure 6.)

Figure 8. Planetary 3-hourly index Kp, magnetic tail field $\overline{F}$ observed by IMP 1, and local disturbance fields at selected magnetic observatories for the period April 11 - May 7, 1964.

Figure 9. Planetary 3-hourly index Kp and RMS deviations of local disturbance fields at selected magnetic observatories for the period April 11 - May 7, 1964. (See Figure 8.)

Figure 10. Planetary 3-hourly index Kp, magnetic tail field $\overline{F}$ observed by IMP 1, and local disturbance fields at selected magnetic observatories for the period May 8 - June 3, 1964.

Figure 11. Planetary 3-hourly index Kp and RMS deviations of local disturbance fields at selected magnetic observatories for the period May 8 - June 3, 1964. (See Figure 10.)

Figure 12. Statistical distribution of the hourly average magnetic tail field magnitude as observed by IMP 1 during the period March 15 - May 29, 1964 for low ($\leq 2-$) and high ($\geq 2$) Kp.

Figure 13. Variations in the horizontal component of the magnetic field at College, Alaska, during five geomagnetic storms occurring while IMP 1 was in the earth's magnetic tail which are discussed in the text. Orbit numbers are indicated to the left of each 3 day trace.

Figure 14. Relative position of the IMP-1 satellite in the Earth's magnetic tail during the April 1, 1964 Geomagnetic Storm.

Figure 15. Correlated magnetic tail field magnitude and direction in solar ecliptic coordinates and local disturbance fields at selected magnetic observatories during the April 1, 1964 geomagnetic storm.

Figure 16. Magnetic field measurements of the Earth's magnetic tail by IMP 1 on orbit no. 33 from March 30 to April 2, 1964. Traversal of the neutral sheet is identified at 9.9 $R_E$ on the inbound portion of the orbit.

Figure 17. Magnetic field measurements of the Earth's magnetic tail by IMP 1 on orbit no. 34 from April 3 to 6, 1964. Indication of near-traversal of neutral sheet on April 6 between 25-23 $R_e$.

Figure 18. Magnetic field measurements of the Earth's magnetic tail by IMP 1 on orbit no. 35 from April 7 to 10, 1964. Indication of near traversal of neutral sheet on April 10 between 22-20 $R_E$.

Figure 19. Relative position of the IMP-1 satellite in the Earth's magnetic tail during the April 27, 1964 geomagnetic storm.

Figure 20. Correlated magnetic tail field magnitude and direction in solar ecliptic coordinates and local disturbance fields at selected magnetic observatories during the April 27, 1964 geomagnetic storm.

Figure 21. Correlated electron flux and magnetic field variations in the tail of the magnetosphere observed by IMP 1 on orbit 40 inbound, April 29, 1964. The neutral sheet was observed during this orbit at a position of 19.8 $R_E$, coincident with an abrupt increase in the electron flux.

Figure 22. Relative position of the IMP-1 satellite in the Earth's magnetic tail during the May 10, 1964 geomagnetic storm.

Figure 23. Correlated magnetic tail field magnitude and direction in solar ecliptic coordinates and local disturbance fields at selected magnetic observatories during the May 10, 1964 geomagnetic storm.

Figure 24. Relative position of the IMP-1 satellite in the Earth's magnetic tail during the May 13, 1964 geomagnetic storm.

Figure 25. Correlated magnetic tail field magnitude and direction in solar ecliptic coordinates and local disturbance fields at selected magnetic observatories during the May 13, 1964 geomagnetic storm.

Figure 26. Relative position of the IMP-1 satellite in the Earth's magnetic tail during the May 23, 1964 geomagnetic storm.

Figure 27. Correlated magnetic tail field magnitude and direction in solar ecliptic coordinates and local disturbance fields at selected magnetic observatories during the May 23, 1964 geomagnetic storm.

Figure 28. Relative positions of the moon and the IMP 1 satellite in the Earth's magnetic tail as seen from the Earth in: a, March, 1964, during orbit no. 32; b, April, 1964, during orbit no. 40; c, May, 1964, during orbit no. 47. The crossed hatched region indicates the position of the solar magnetosphere equatorial plane during each time period. IMP-1 and the Moon are aligned in a $X_{se}$ - $Z_{se}$ plane ("full" moon for the IMP-1) on: a. 29 March 1135 UT, b. 26 April 1535 UT and c. 25 May 0945 UT.

# RESULTS OF IMP-1 MAGNETIC FIELD EXPERIMENT

(11/27/63 TO 5/31/64)

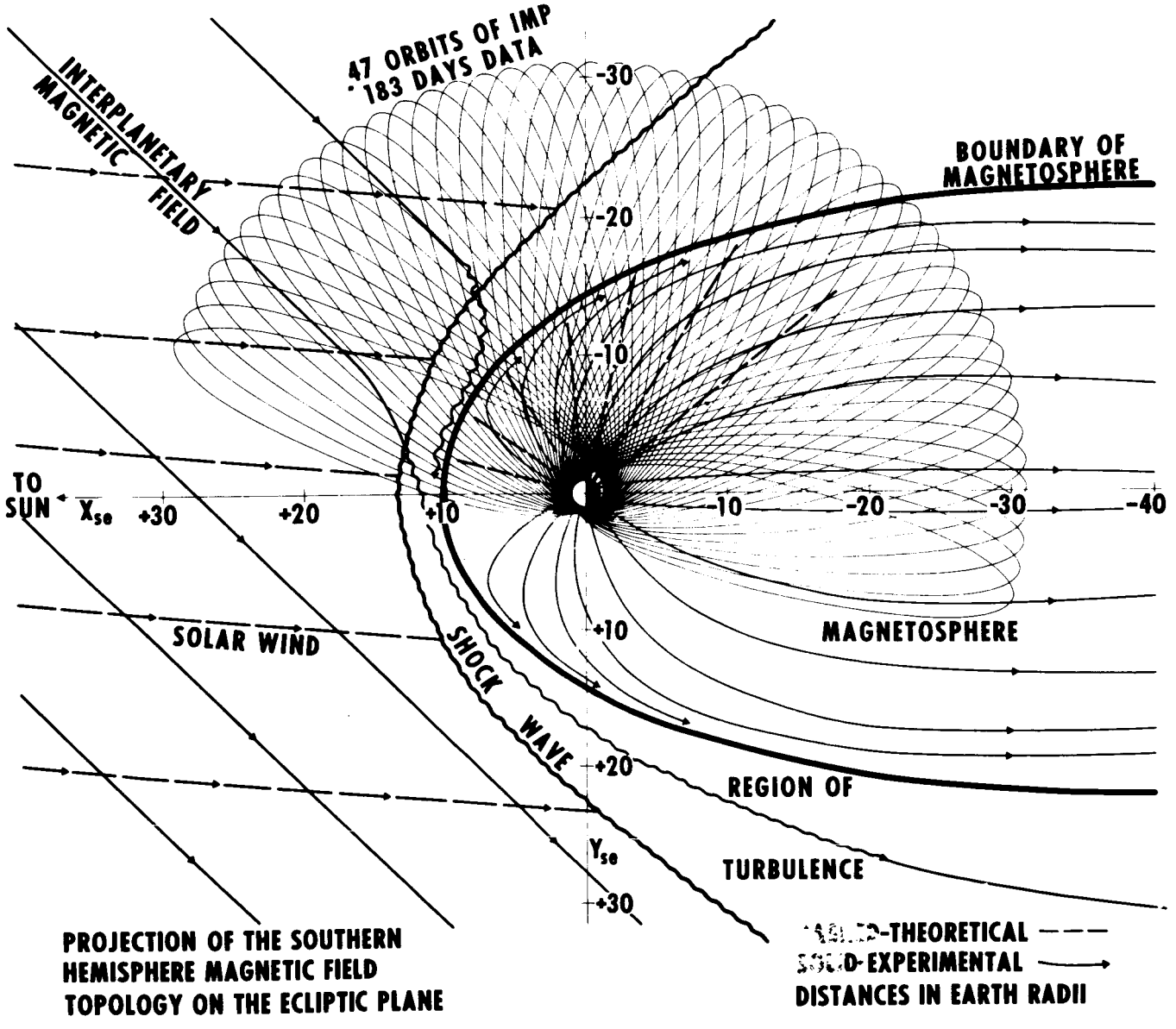


Figure 1

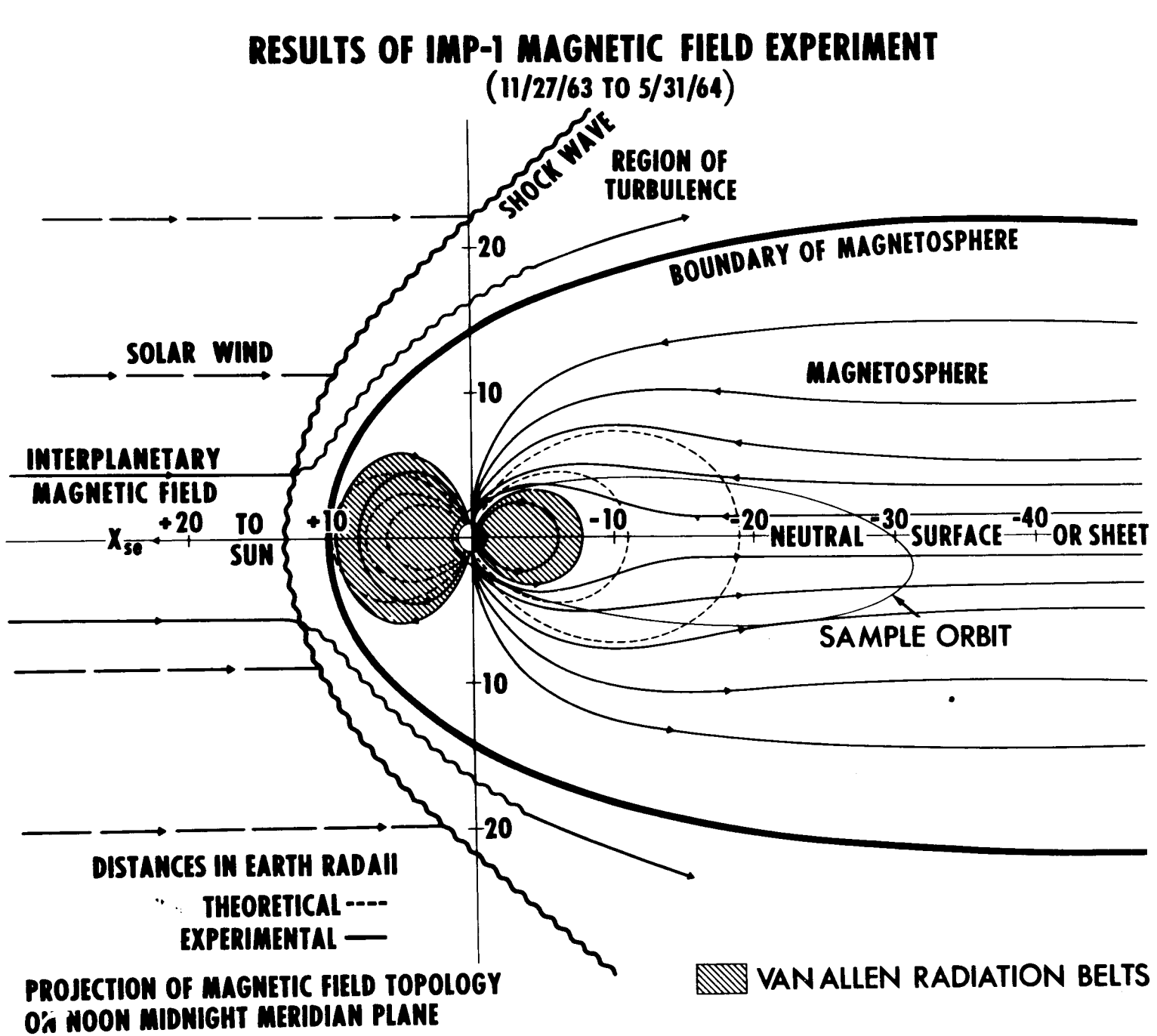
RESULTS OF IMP-1 MAGNETIC FIELD EXPERIMENT
(11/27/63 TO 5/31/64)
SHOCK WAVE
REGION OF TURBULENCE
BOUNDARY OF MAGNETOSPHERE
SOLAR WIND
MAGNETOSPHERE
INTERPLANETARY MAGNETIC FIELD
$X_{se}$
+20
+10
-10
-20
-30
-40
TO SUN
NEUTRAL SURFACE OR SHEET
SAMPLE ORBIT
20
10
10
20
DISTANCES IN EARTH RADII
THEORETICAL ----
EXPERIMENTAL ——
PROJECTION OF MAGNETIC FIELD TOPOLOGY
ON NOON MIDNIGHT MERIDIAN PLANE
VAN ALLEN RADIATION BELTS

Figure 2

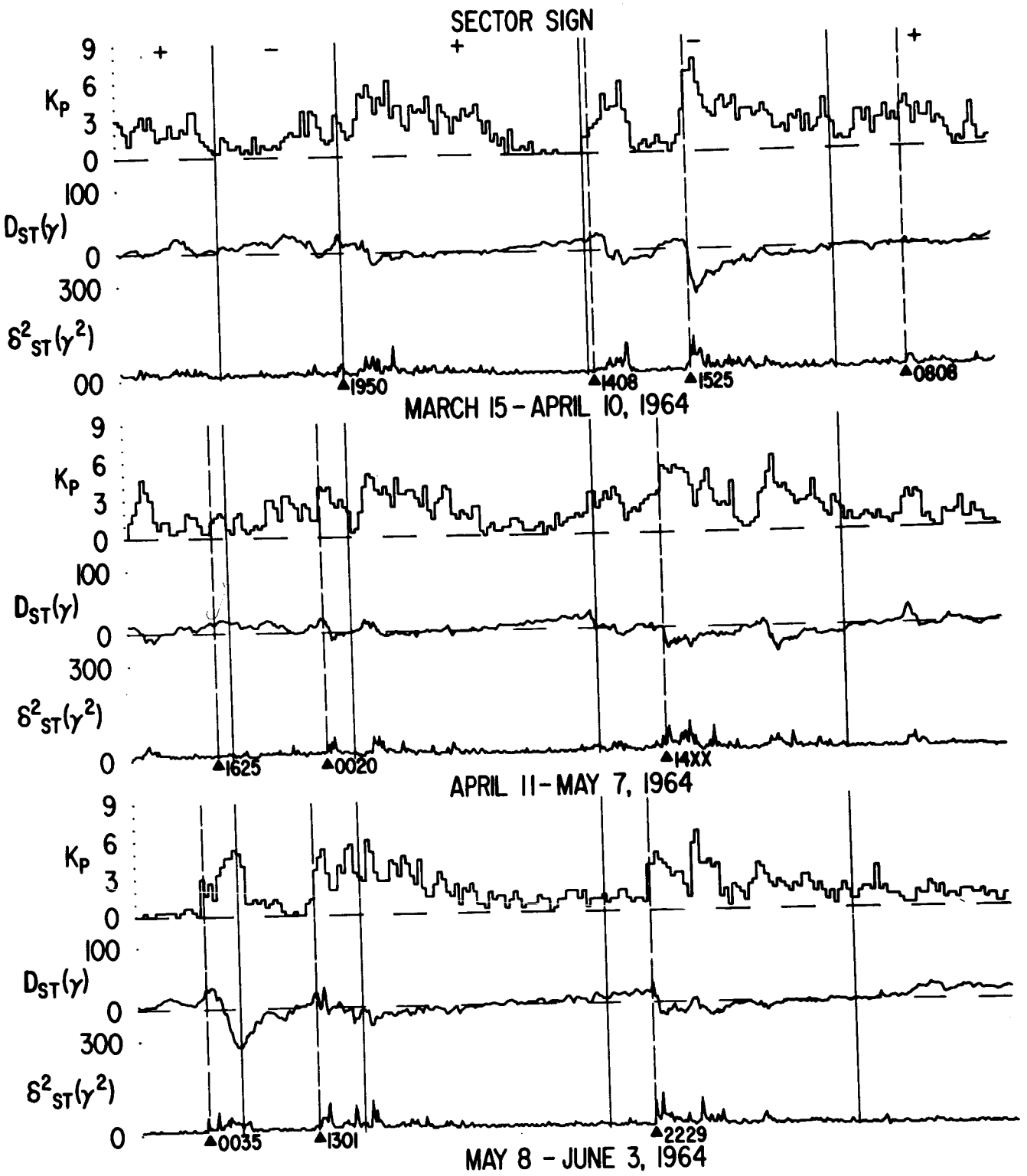
SECTOR SIGN
+
−
+
−
+
9
6
3
0
$K_P$
100
0
$D_{ST}(\gamma)$
300
0
$\delta^2_{ST}(\gamma^2)$
00
▲1950
▲1408
▲1525
▲0808
MARCH 15 - APRIL 10, 1964
9
6
3
0
$K_P$
100
0
$D_{ST}(\gamma)$
300
0
$\delta^2_{ST}(\gamma^2)$
0
▲1625
▲0020
▲14XX
APRIL 11 - MAY 7, 1964
9
6
3
0
$K_P$
100
0
$D_{ST}(\gamma)$
300
0
$\delta^2_{ST}(\gamma^2)$
0
▲0035
▲1301
▲2229
MAY 8 - JUNE 3, 1964

Figure 3

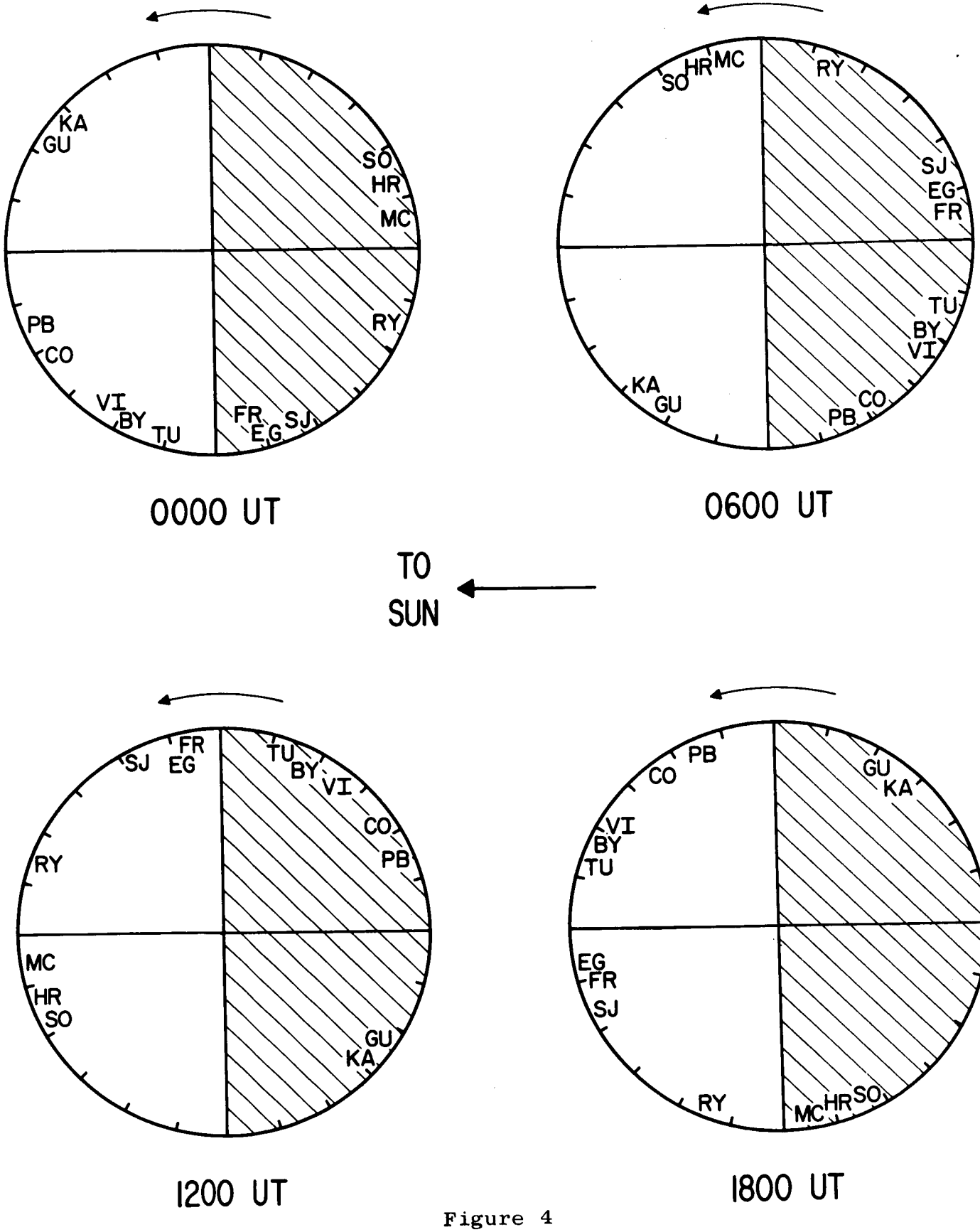
KA
GU
SO
HR
MC
PB
CO
VI
BY
TU
FR
EG
SJ
RY
0000 UT
SO
HR
MC
RY
SJ
EG
FR
TU
BY
VI
KA
GU
CO
PB
0600 UT
TO
SUN
SJ
FR
EG
TU
BY
VI
CO
PB
RY
MC
HR
SO
GU
KA
1200 UT
PB
CO
VI
BY
TU
GU
KA
EG
FR
SJ
RY
MC
HR
SO
1800 UT

Figure 4

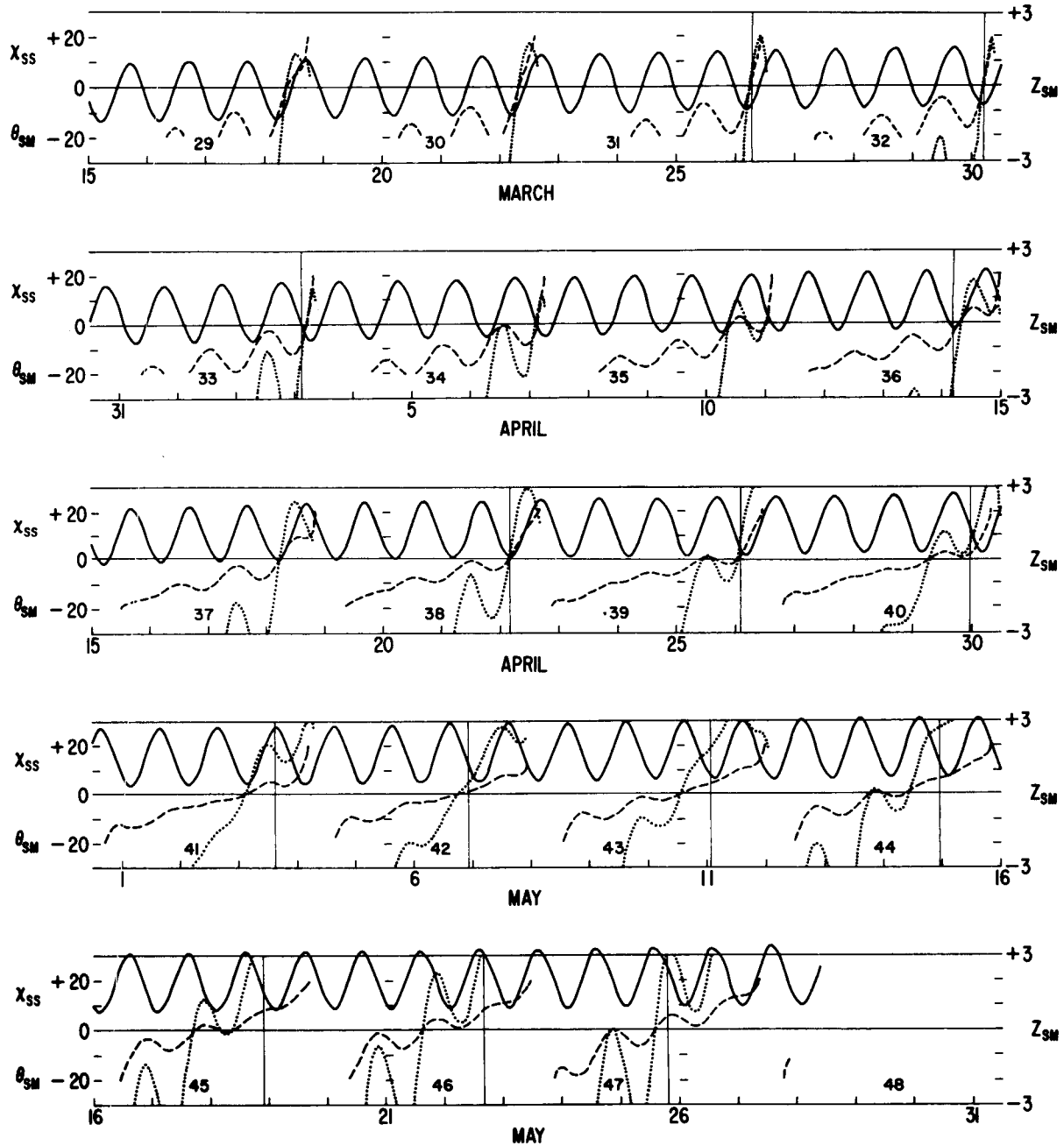
$X_{SS}$
+20
0
−20
$\theta_{SM}$
+3
−3
$Z_{SM}$
29
30
31
32
15
20
25
30
MARCH
33
34
35
36
31
5
10
15
APRIL
37
38
39
40
15
20
25
30
APRIL
41
42
43
44
1
6
11
16
MAY
45
46
47
48
16
21
26
31
MAY

Figure 5

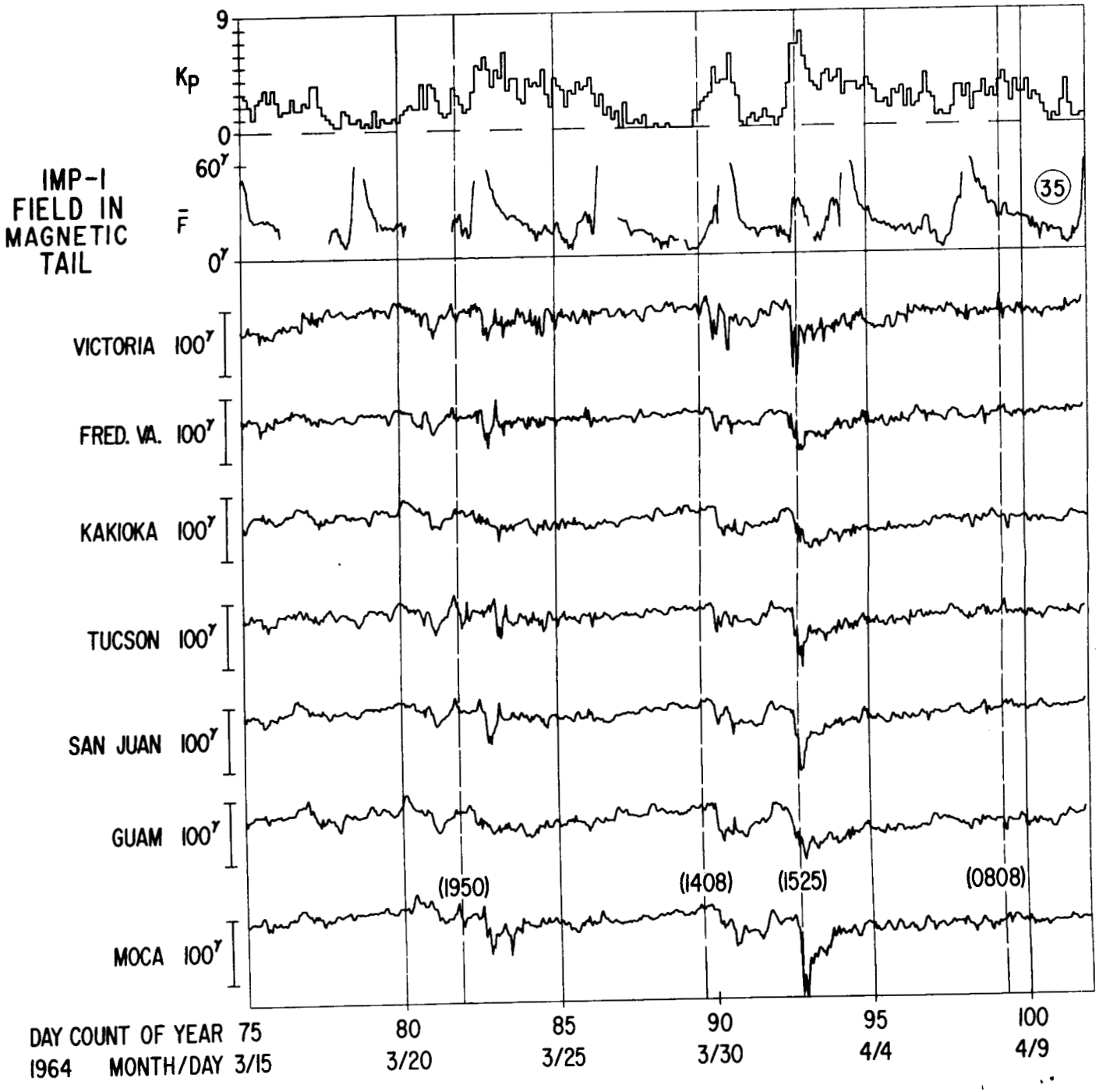
IMP-I
FIELD IN
MAGNETIC
TAIL
9
$K_P$
0
60γ
F
0γ
35
VICTORIA 100γ
FRED. VA. 100γ
KAKIOKA 100γ
TUCSON 100γ
SAN JUAN 100γ
GUAM 100γ
MOCA 100γ
(1950)
(1408)
(1525)
(0808)
DAY COUNT OF YEAR 75 80 85 90 95 100
1964 MONTH/DAY 3/15 3/20 3/25 3/30 4/4 4/9

Figure 5

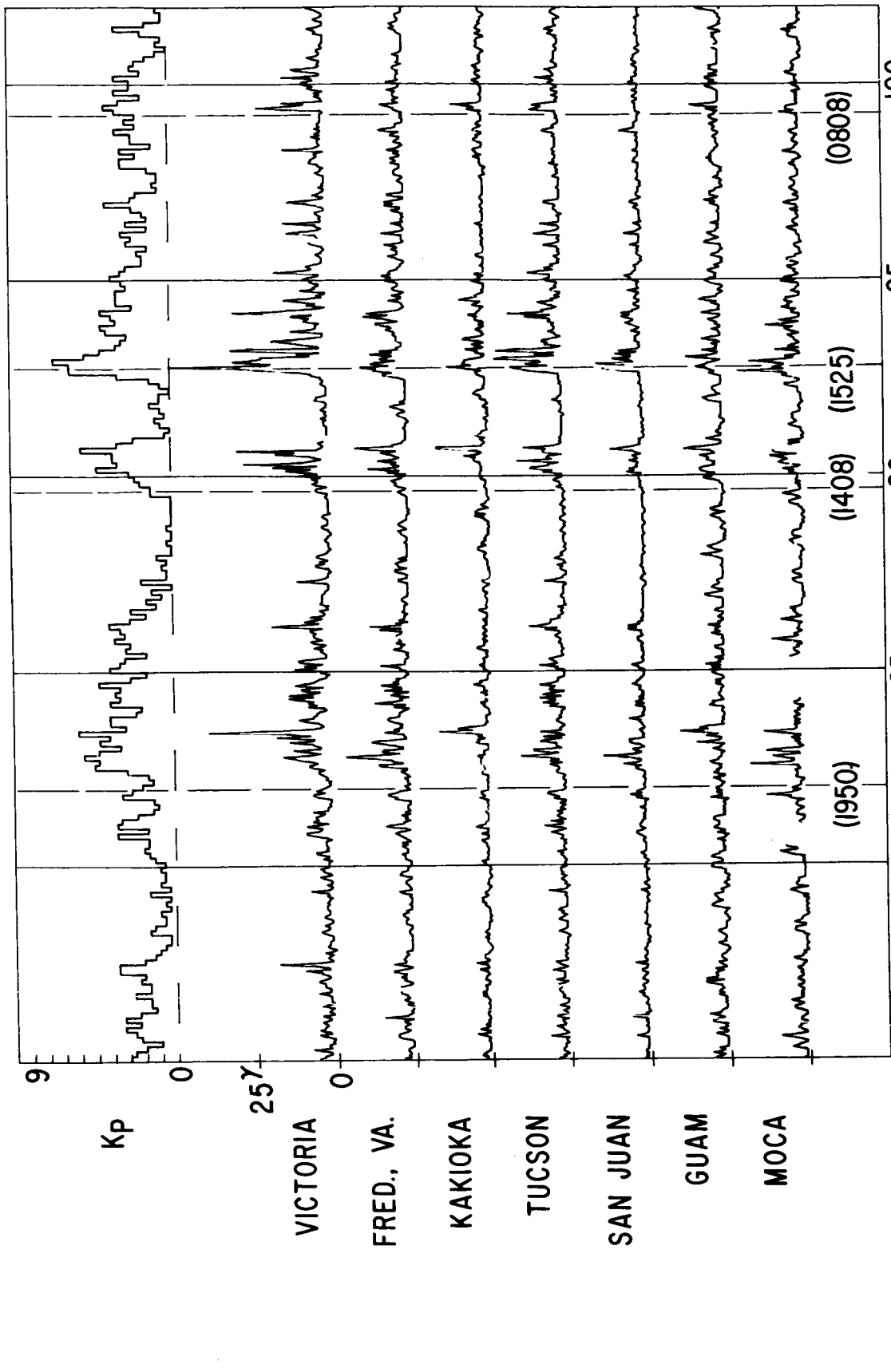
Kp
9
0
25γ
0
VICTORIA
FRED., VA.
KAKIOKA
TUCSON
SAN JUAN
GUAM
MOCA
(1950)
(1408)
(1525)
(0808)
DAY COUNT OF YEAR
1964 MONTH/DAY
75
3/15
80
3/20
85
3/25
90
3/30
95
4/4
100
4/9

Figure 7

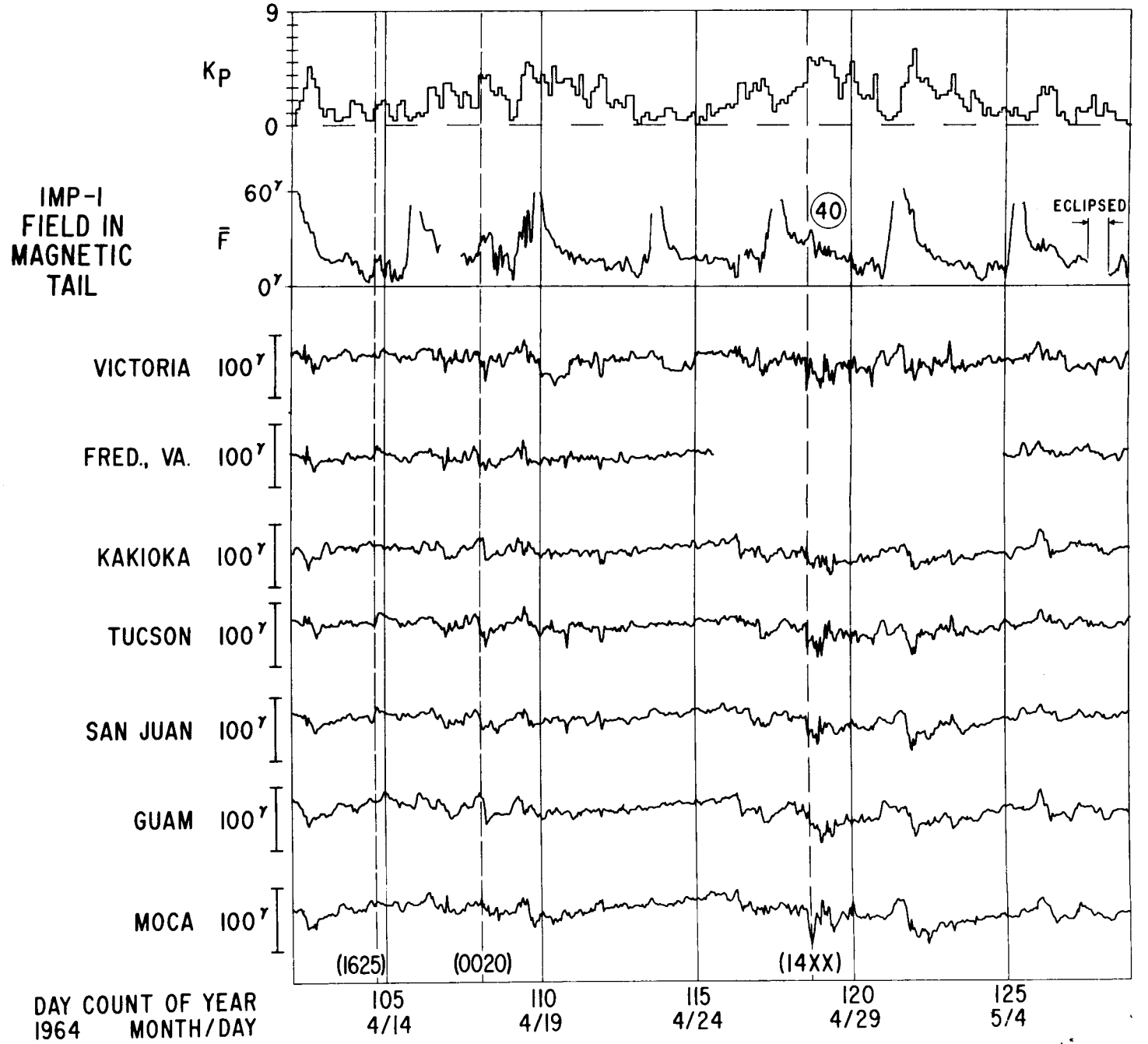
9
$K_P$
0
IMP-I
FIELD IN
MAGNETIC
TAIL
60γ
$\bar{F}$
0γ
40
ECLIPSED
VICTORIA 100γ
FRED., VA. 100γ
KAKIOKA 100γ
TUCSON 100γ
SAN JUAN 100γ
GUAM 100γ
MOCA 100γ
(1625)
(0020)
(14XX)
DAY COUNT OF YEAR
1964 MONTH/DAY
105
4/14
110
4/19
115
4/24
120
4/29
125
5/4

Figure 8

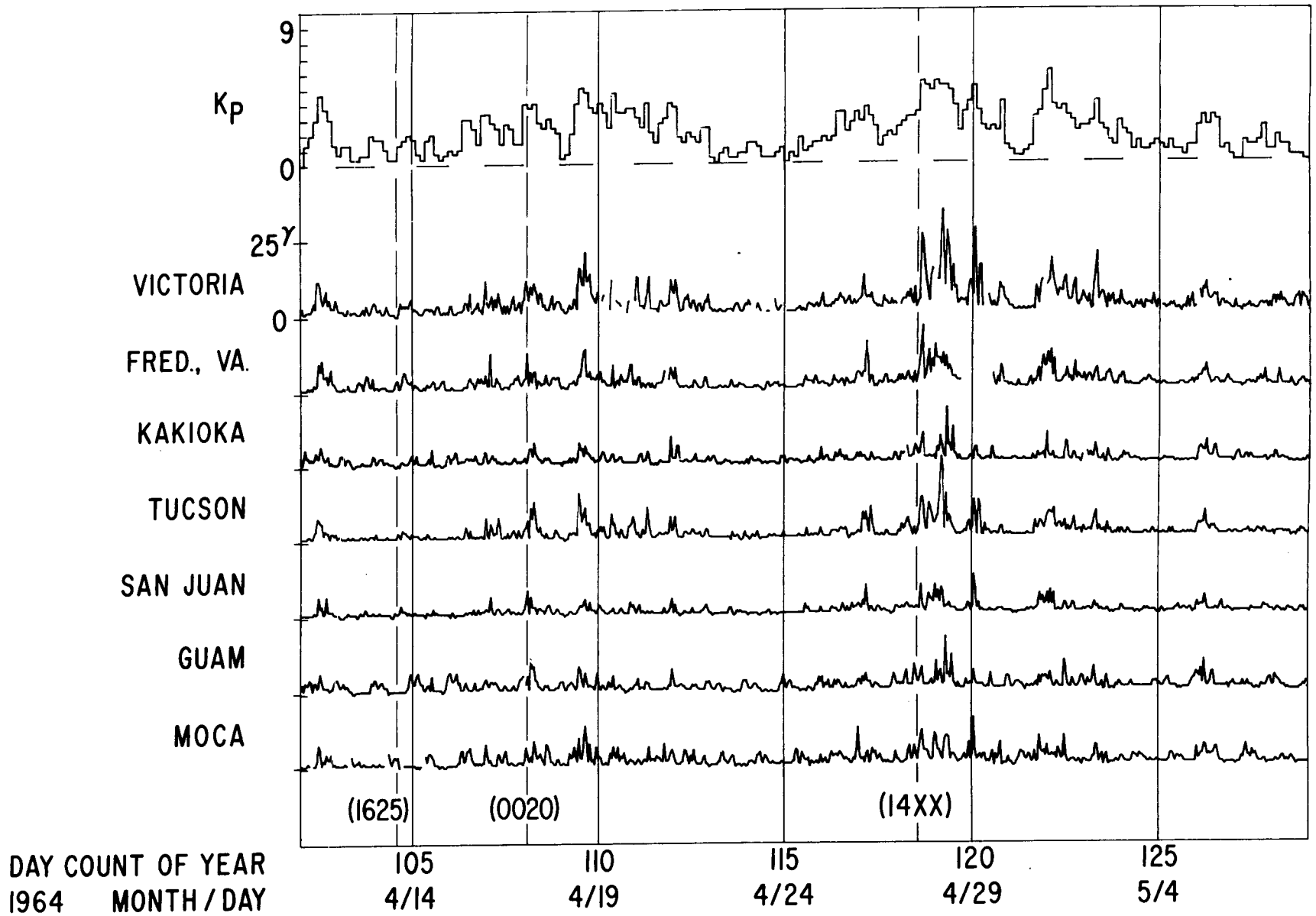
9
Kp
0
25γ
0
VICTORIA
FRED., VA.
KAKIOKA
TUCSON
SAN JUAN
GUAM
MOCA
(1625)
(0020)
(14XX)
DAY COUNT OF YEAR
1964 MONTH / DAY
105
4/14
110
4/19
115
4/24
120
4/29
125
5/4

Figure 9

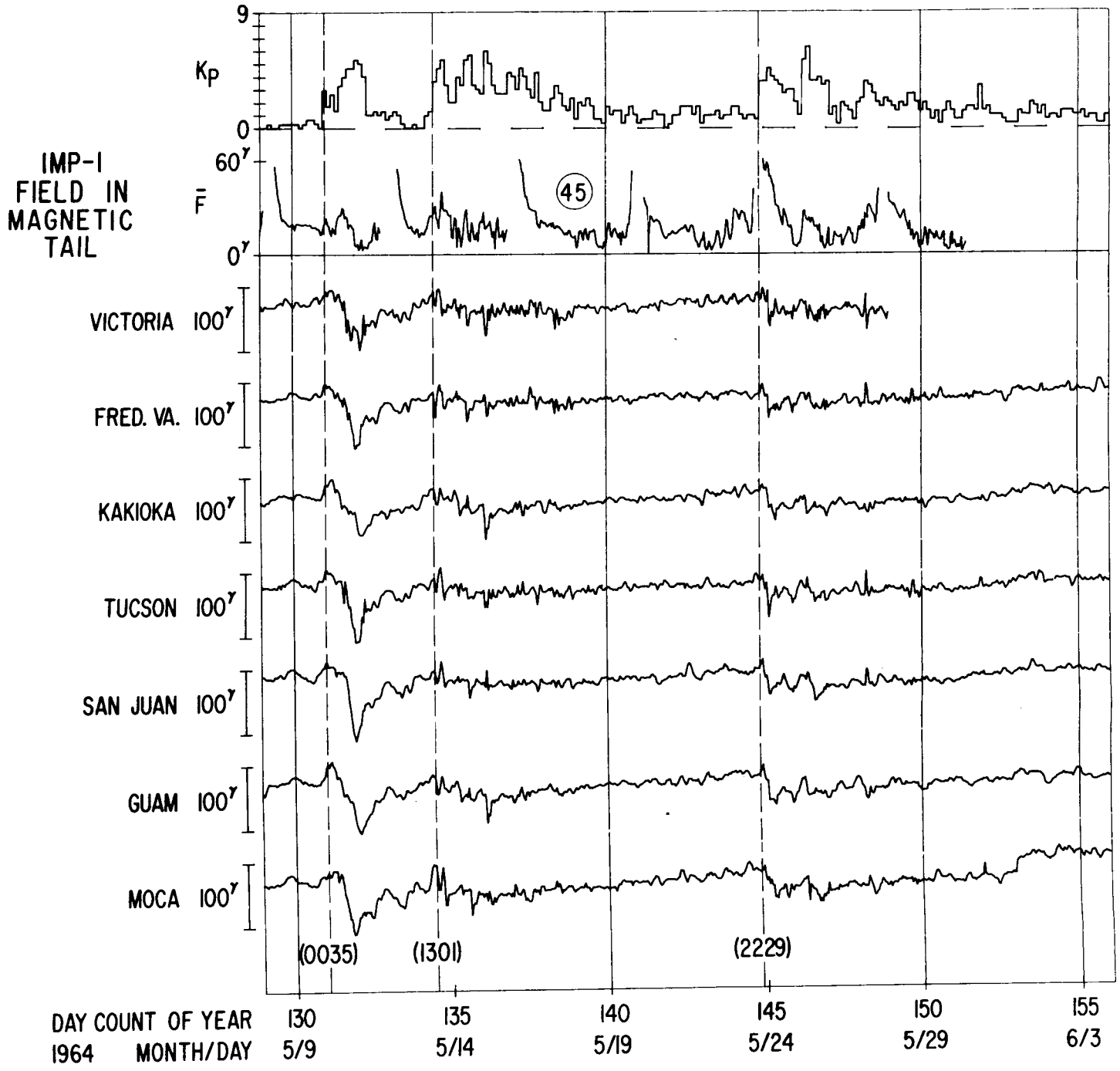
9
Kp
0
IMP-I
FIELD IN
MAGNETIC
TAIL
60γ
F
0γ
45
VICTORIA 100γ
FRED. VA. 100γ
KAKIOKA 100γ
TUCSON 100γ
SAN JUAN 100γ
GUAM 100γ
MOCA 100γ
(0035)
(1301)
(2229)
DAY COUNT OF YEAR
1964 MONTH/DAY
130
5/9
135
5/14
140
5/19
145
5/24
150
5/29
155
6/3

Figure 10

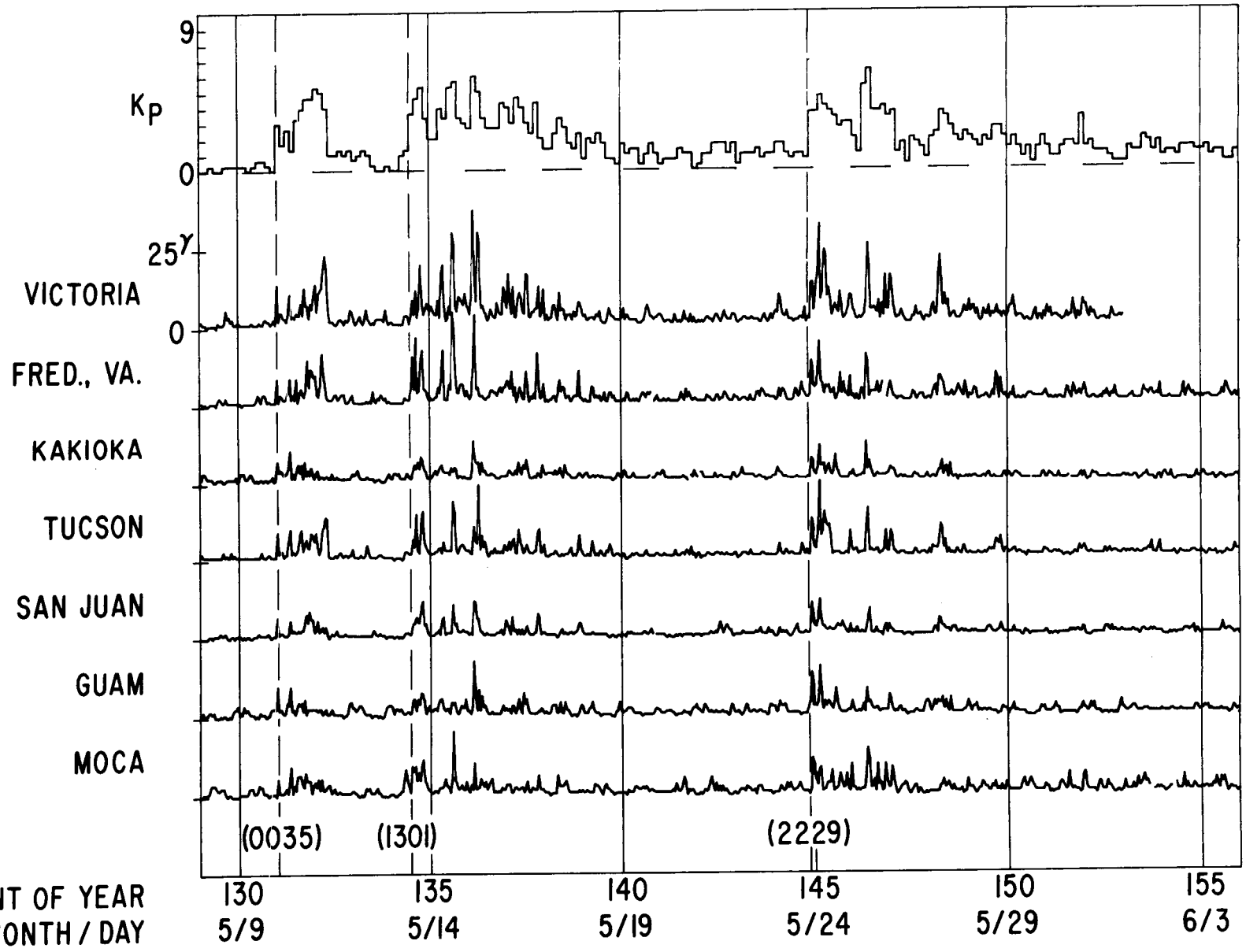
9
$K_P$
0
25γ
VICTORIA
0
FRED., VA.
KAKIOKA
TUCSON
SAN JUAN
GUAM
MOCA
(0035)
(1301)
(2229)
DAY COUNT OF YEAR
1964 MONTH / DAY
130
5/9
135
5/14
140
5/19
145
5/24
150
5/29
155
6/3

Figure 11

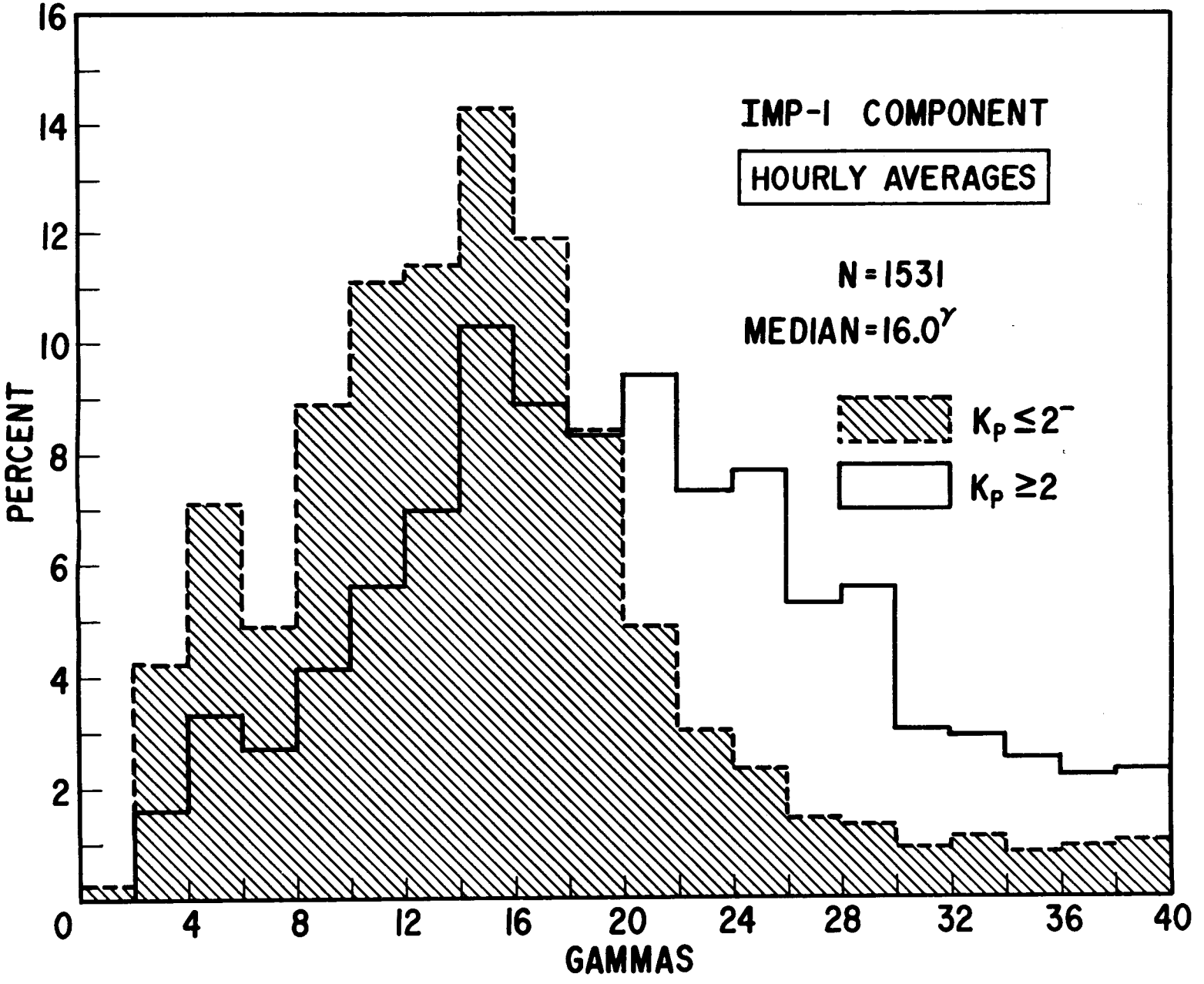


Figure 12

DISTRIBUTION OF MAGNETIC TAIL FIELD MAGNITUDE

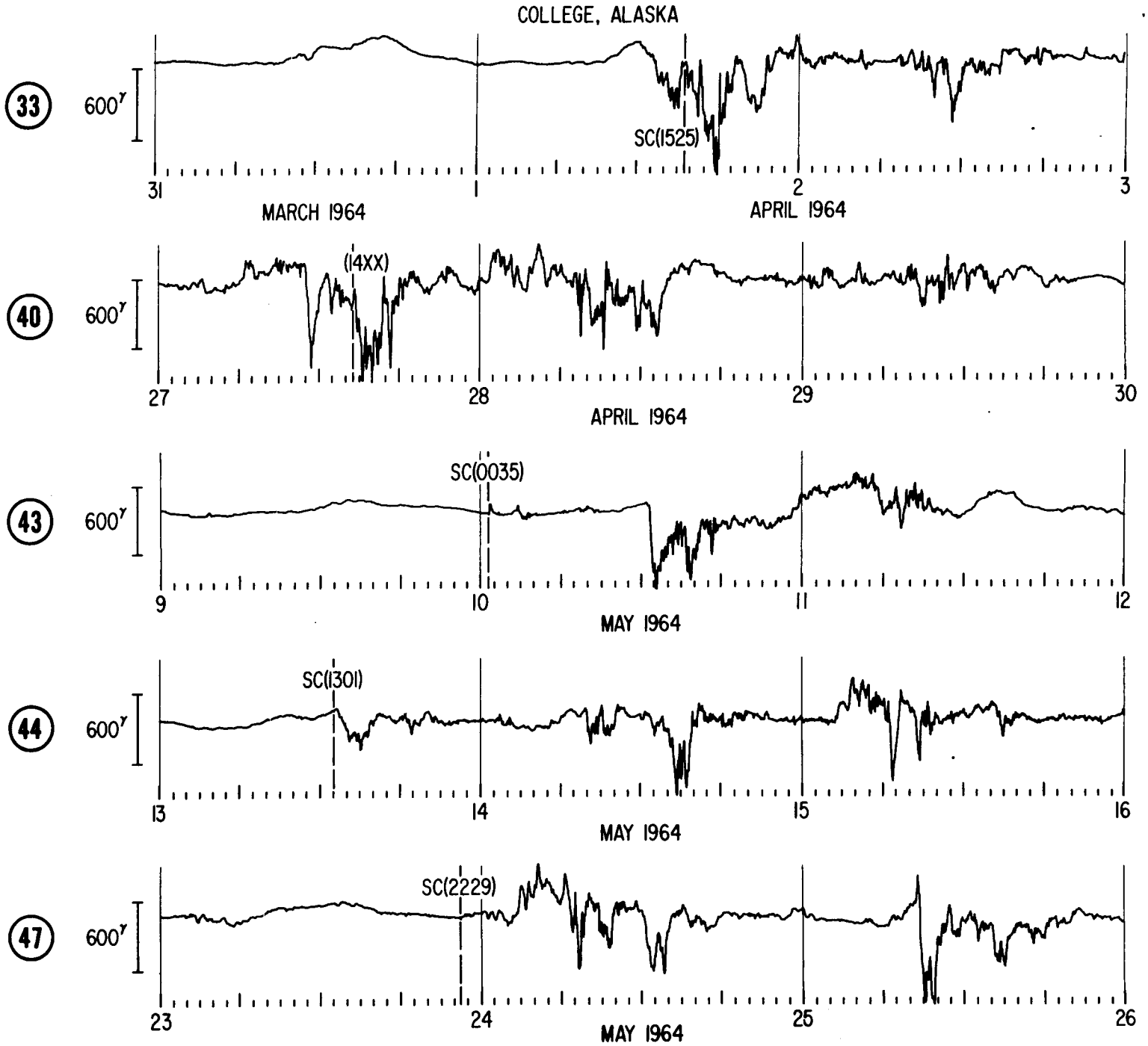
COLLEGE, ALASKA
33
600γ
SC(1525)
31
2
3
MARCH 1964
APRIL 1964
40
600γ
(14XX)
27
28
29
30
APRIL 1964
43
600γ
SC(0035)
9
10
11
12
MAY 1964
44
600γ
SC(1301)
13
14
15
16
MAY 1964
47
600γ
SC(2229)
23
24
25
26
MAY 1964

Figure 13

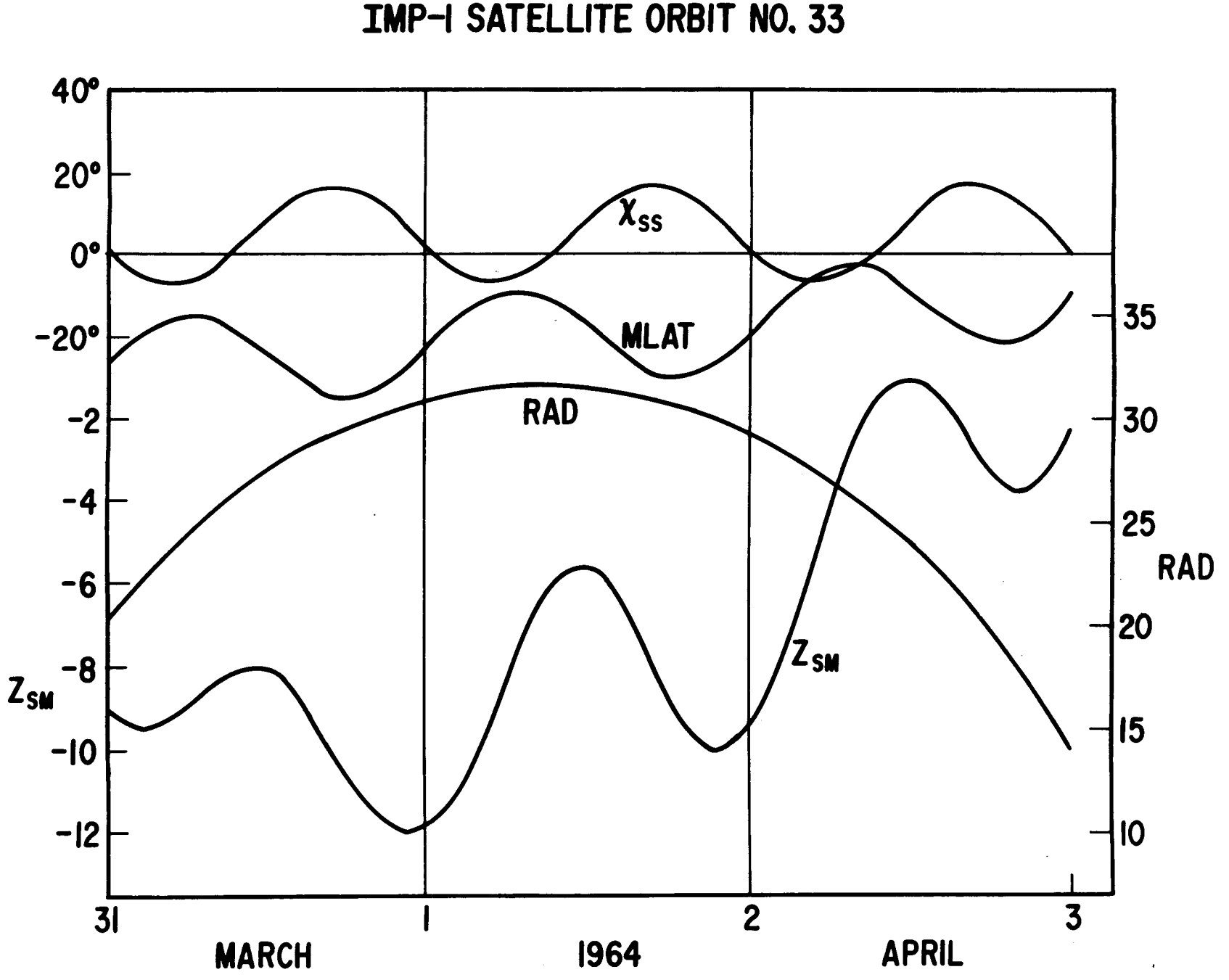
IMP-I SATELLITE ORBIT NO. 33
40°
20°
0°
-20°
-2
-4
-6
-8
-10
-12
$Z_{SM}$
$\chi_{SS}$
MLAT
RAD
$Z_{SM}$
35
30
25
20
15
10
RAD
31
MARCH
1
1964
2
APRIL
3

Figure 14

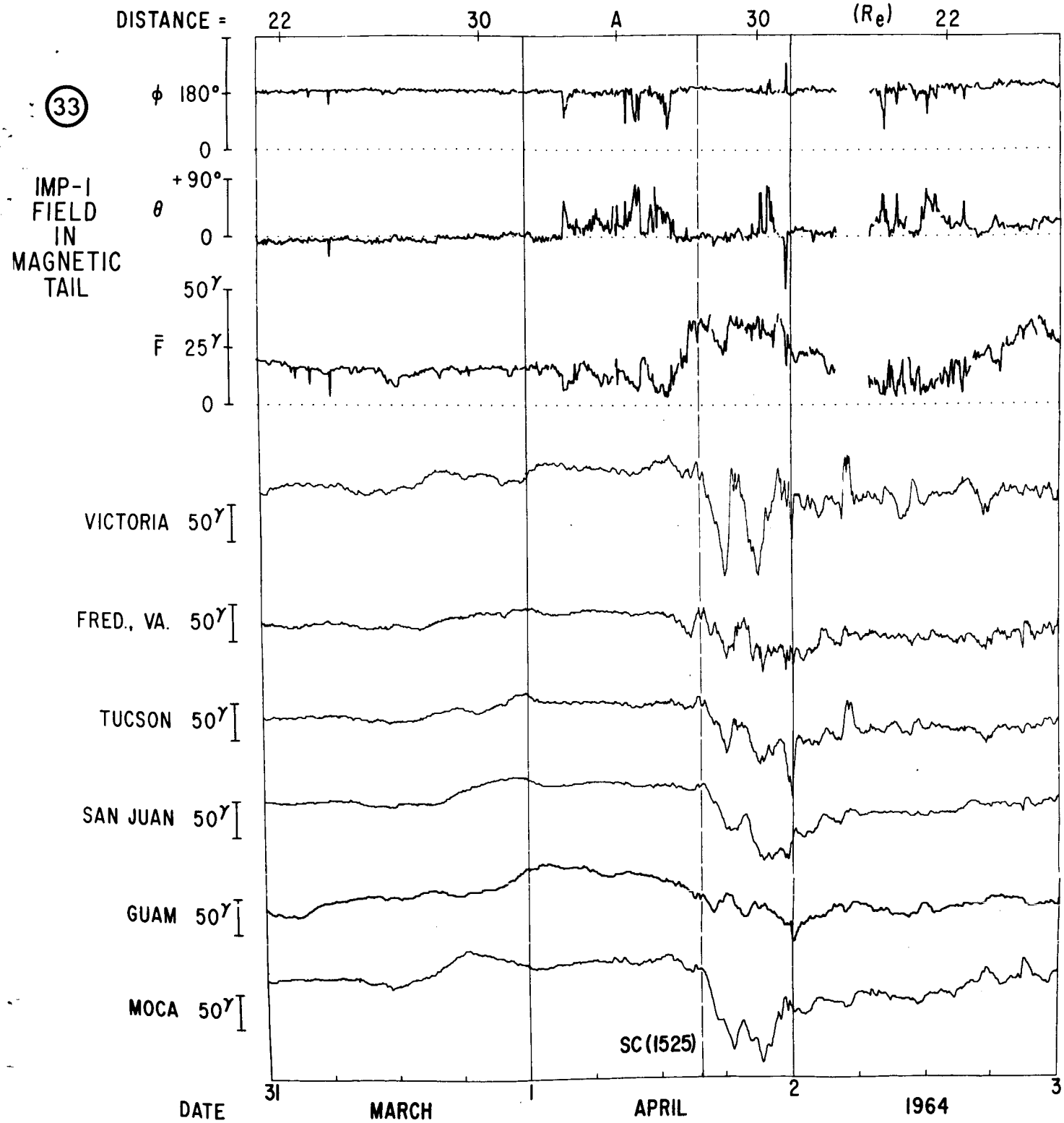
DISTANCE = 22 30 A 30 (Re) 22
33
IMP-I FIELD IN MAGNETIC TAIL
φ 180° 0
θ +90° 0
F̄ 50γ 25γ 0
VICTORIA 50γ
FRED., VA. 50γ
TUCSON 50γ
SAN JUAN 50γ
GUAM 50γ
MOCA 50γ
SC (1525)
DATE 31 MARCH 1 APRIL 2 3 1964

Figure 15

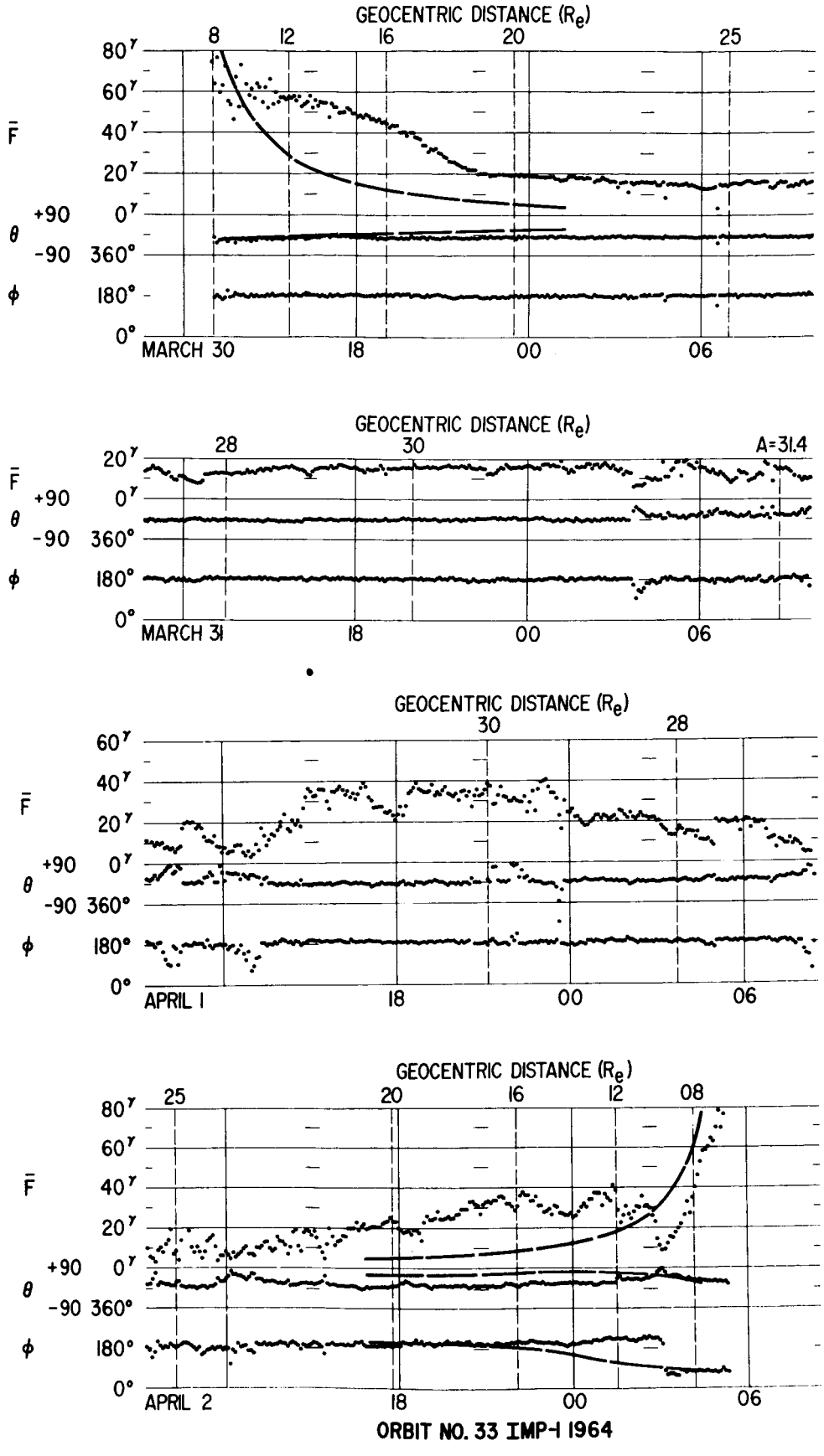
GEOCENTRIC DISTANCE ($R_e$)
8
12
16
20
25
80γ
60γ
40γ
20γ
0γ
$\bar{F}$
+90
$\theta$
-90
360°
$\phi$
180°
0°
MARCH 30
18
00
06
GEOCENTRIC DISTANCE ($R_e$)
28
30
A=31.4
20γ
0γ
$\bar{F}$
+90
$\theta$
-90
360°
$\phi$
180°
0°
MARCH 31
18
00
06
GEOCENTRIC DISTANCE ($R_e$)
30
28
60γ
40γ
20γ
0γ
$\bar{F}$
+90
$\theta$
-90
360°
$\phi$
180°
0°
APRIL 1
18
00
06
GEOCENTRIC DISTANCE ($R_e$)
25
20
16
12
08
80γ
60γ
40γ
20γ
0γ
$\bar{F}$
+90
$\theta$
-90
360°
$\phi$
180°
0°
APRIL 2
18
00
06
ORBIT NO. 33 IMP-1 1964

Figure 16

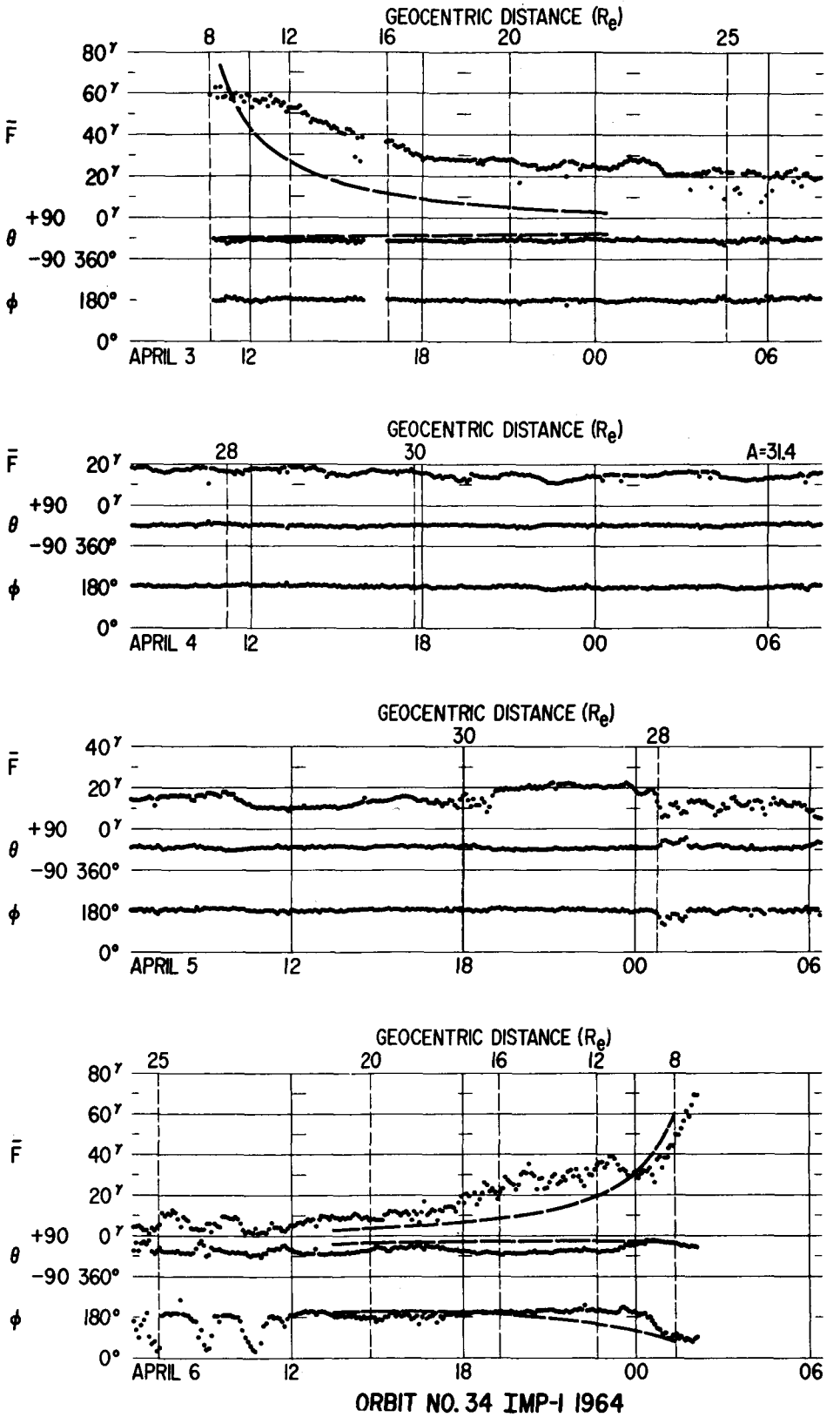
GEOCENTRIC DISTANCE ($R_e$)
8
12
16
20
25
80γ
60γ
40γ
20γ
0γ
$\bar{F}$
+90
θ
-90
360°
φ
180°
0°
APRIL 3
12
18
00
06
GEOCENTRIC DISTANCE ($R_e$)
28
30
A=31.4
20γ
0γ
+90
θ
-90
360°
φ
180°
0°
APRIL 4
12
18
00
06
GEOCENTRIC DISTANCE ($R_e$)
30
28
40γ
20γ
0γ
+90
θ
-90
360°
φ
180°
0°
APRIL 5
12
18
00
06
GEOCENTRIC DISTANCE ($R_e$)
25
20
16
12
8
80γ
60γ
40γ
20γ
0γ
+90
θ
-90
360°
φ
180°
0°
APRIL 6
12
18
00
06
ORBIT NO. 34 IMP-I 1964

Figure 17

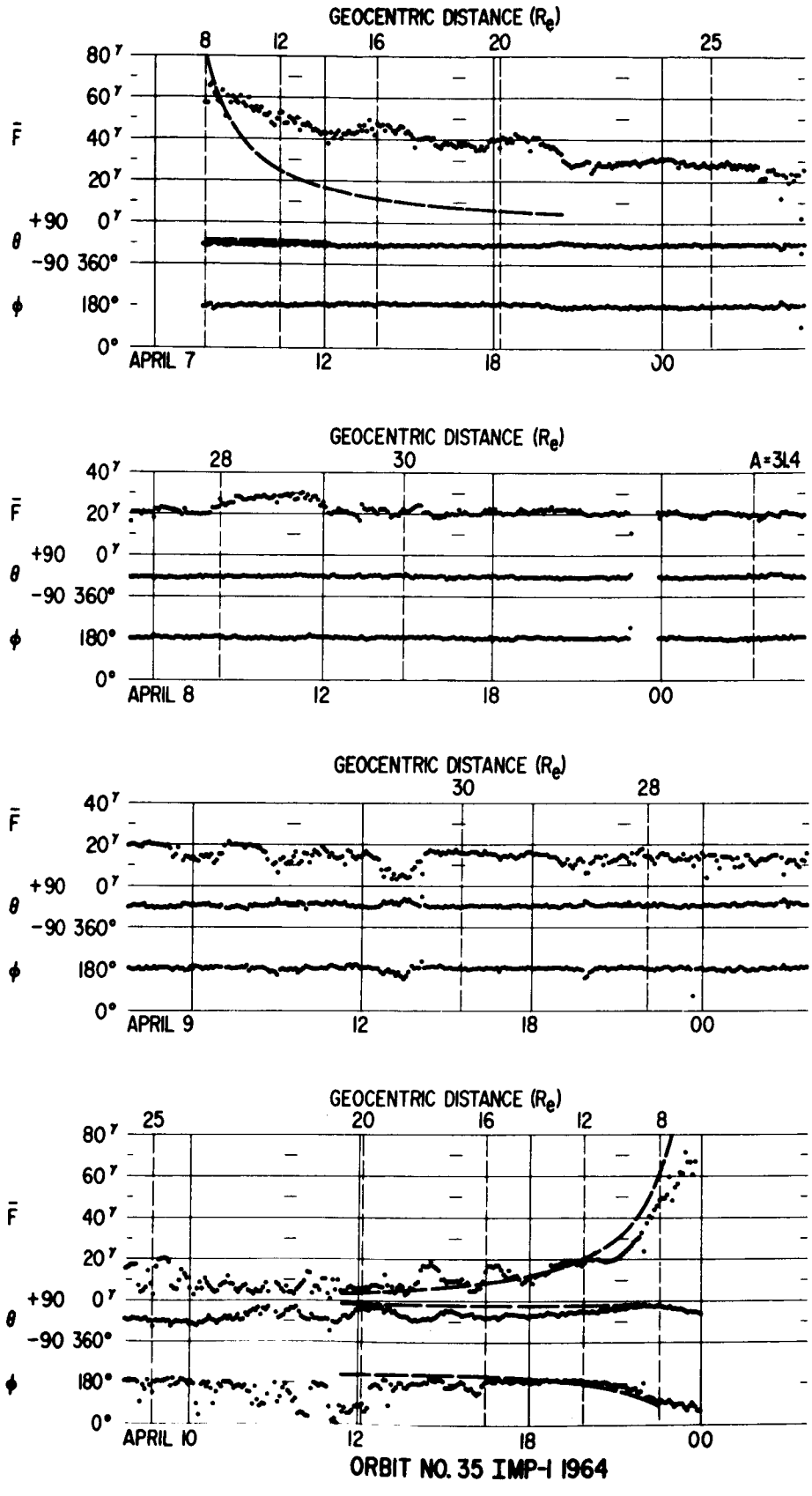
GEOCENTRIC DISTANCE ($R_e$)
8
12
16
20
25
80γ
60γ
40γ
20γ
0γ
+90
θ
-90
360°
φ
180°
0°
APRIL 7
12
18
00
GEOCENTRIC DISTANCE ($R_e$)
28
30
A=3L4
APRIL 8
GEOCENTRIC DISTANCE ($R_e$)
30
28
APRIL 9
GEOCENTRIC DISTANCE ($R_e$)
25
20
16
12
8
APRIL 10
ORBIT NO. 35 IMP-1 1964

Figure 18

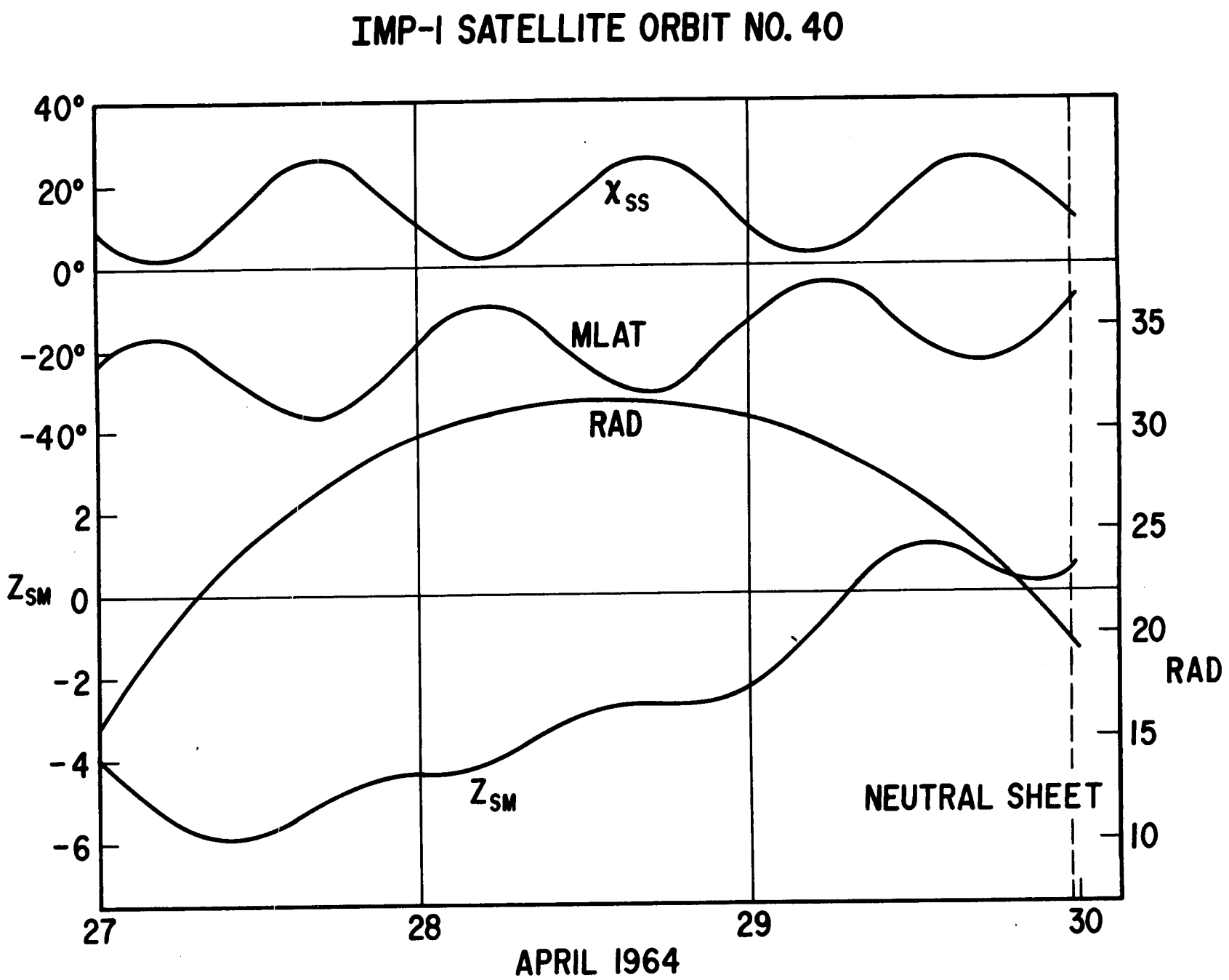
IMP-I SATELLITE ORBIT NO. 40
40°
20°
0°
-20°
-40°
$X_{SS}$
MLAT
RAD
2
$Z_{SM}$ 0
-2
-4
-6
$Z_{SM}$
NEUTRAL SHEET
35
30
25
20
15
10
RAD
27
28
29
30
APRIL 1964

Figure 19

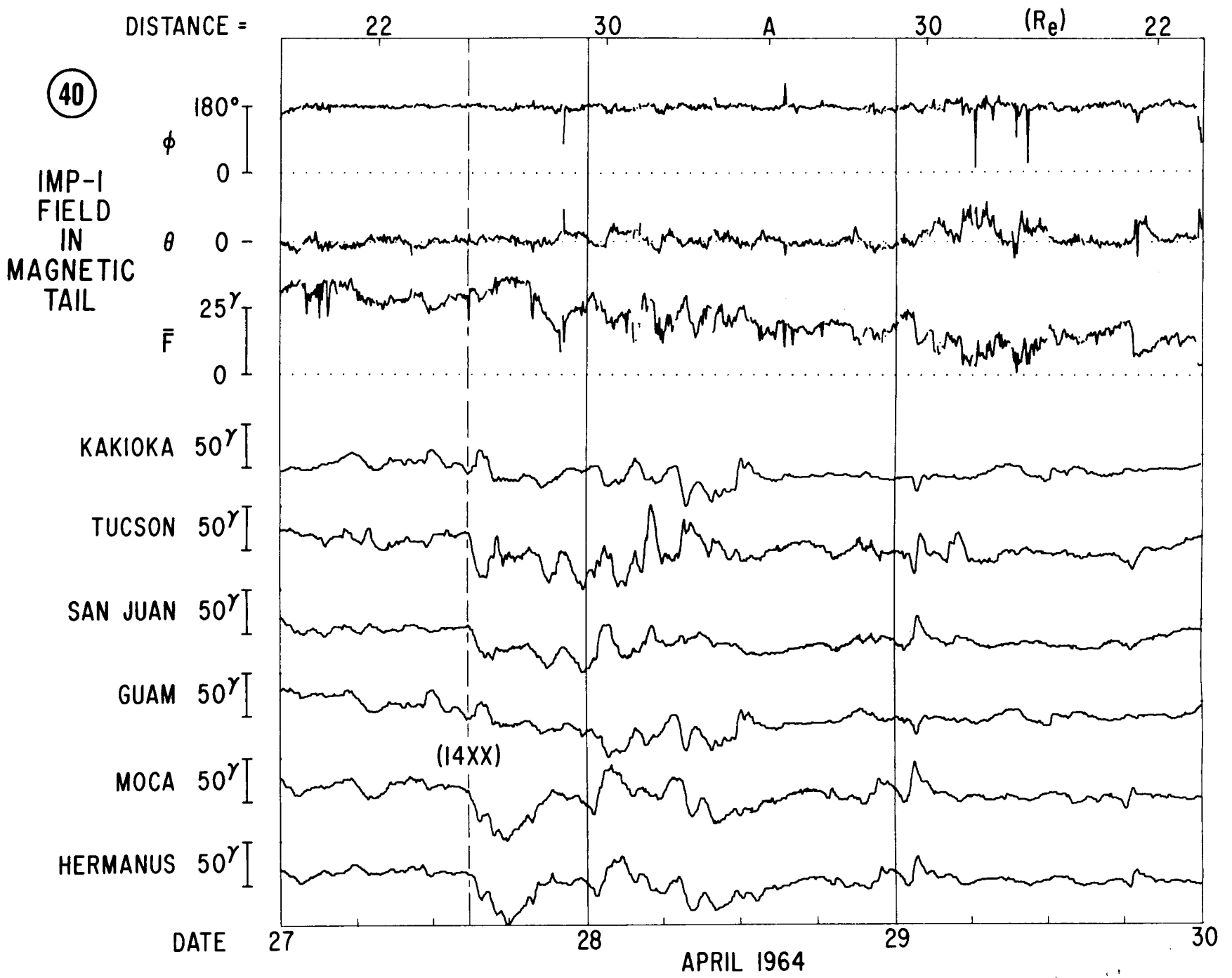
DISTANCE =
22
30
A
30
(Re)
22
40
IMP-I
FIELD
IN
MAGNETIC
TAIL
180°
φ
0
θ
0
25γ
F
0
KAKIOKA 50γ
TUCSON 50γ
SAN JUAN 50γ
GUAM 50γ
(14XX)
MOCA 50γ
HERMANUS 50γ
DATE
27
28
29
30
APRIL 1964

Figure 20

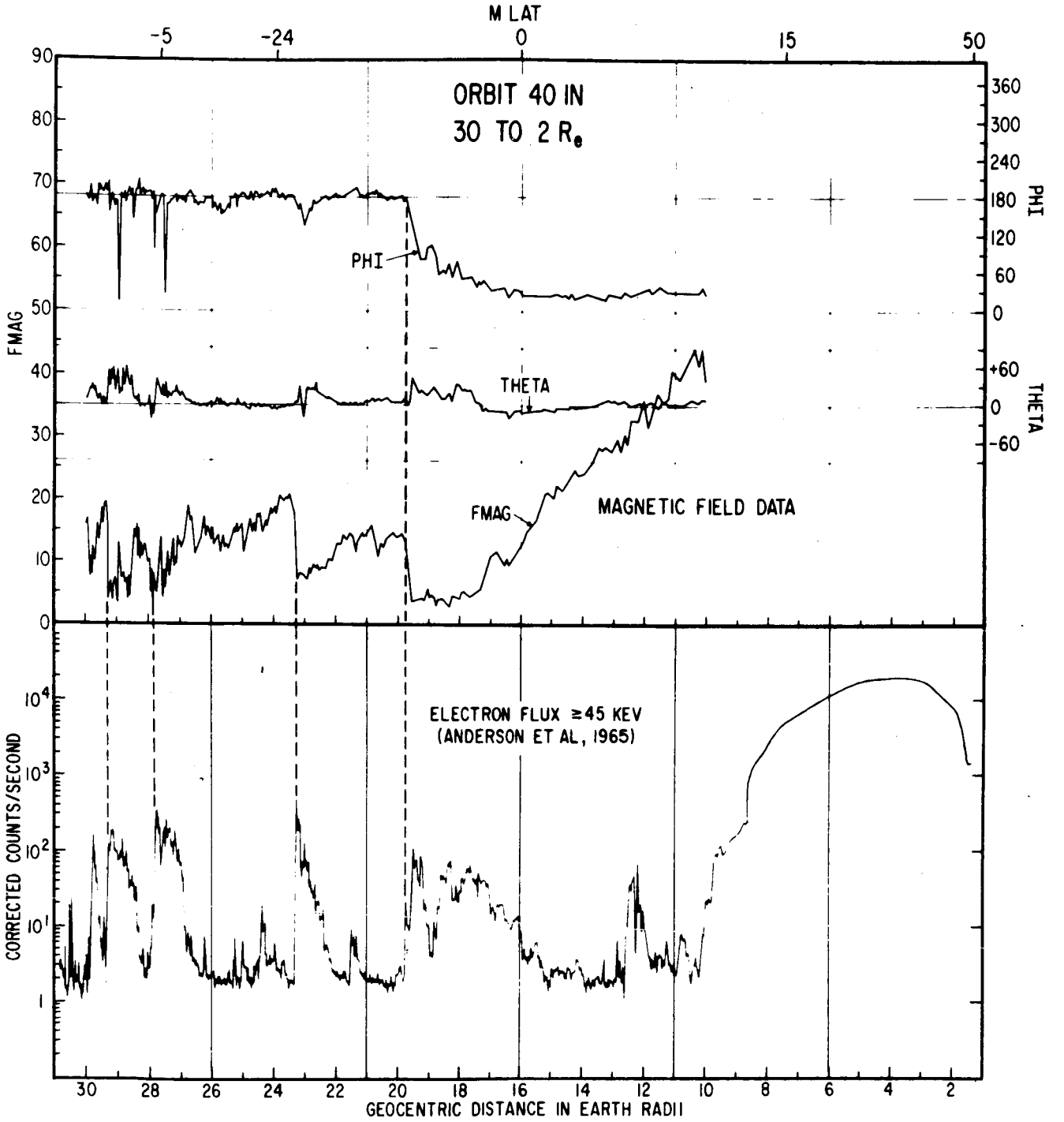


CORRELATED IMP-I MAGNETIC FIELD AND ENERGETIC ELECTRON FLUX IN MAGNETOSPHERIC TAIL

Figure 21

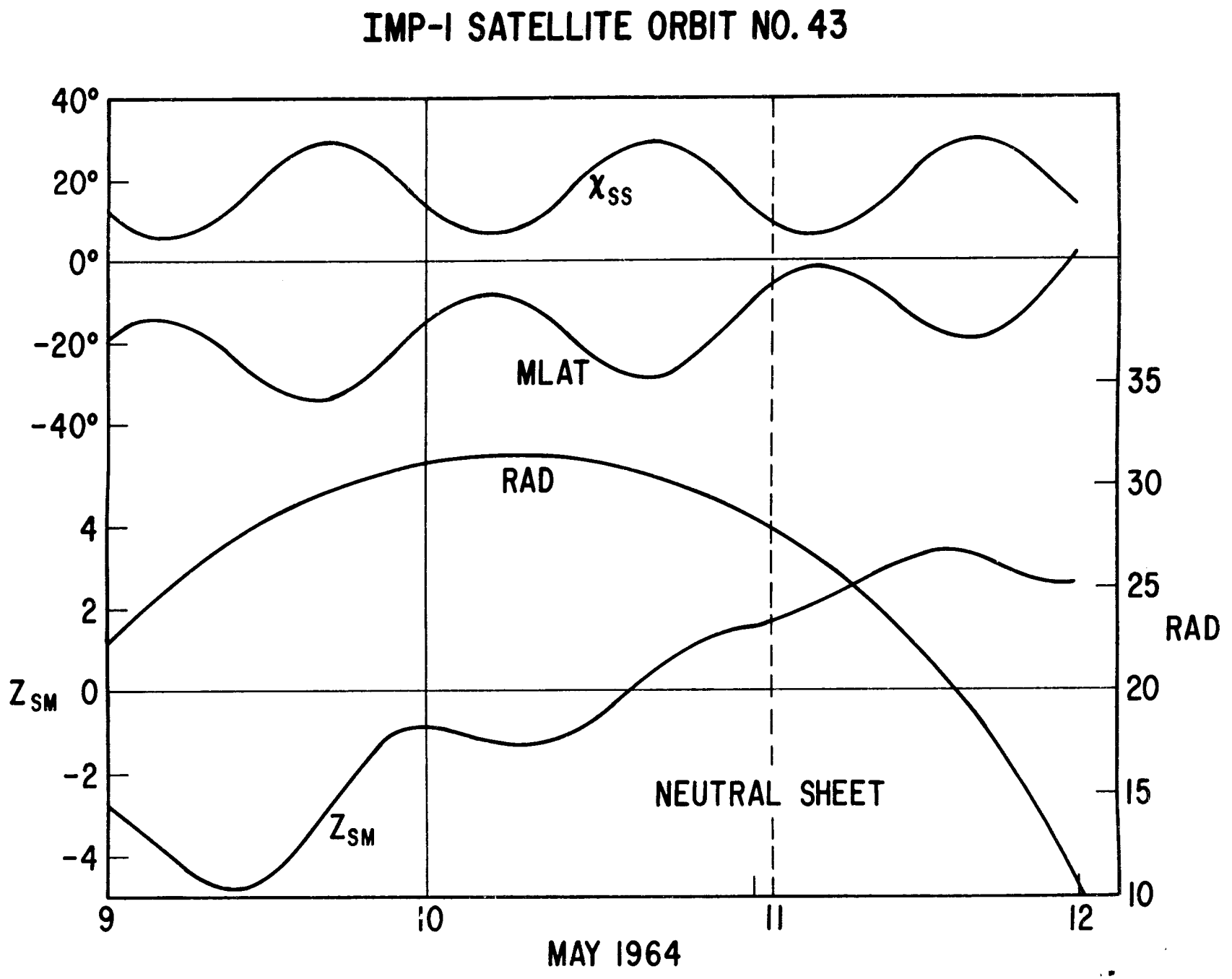
IMP-I SATELLITE ORBIT NO. 43
40°
20°
0°
-20°
-40°
$X_{SS}$
MLAT
RAD
4
2
0
-2
-4
$Z_{SM}$
$Z_{SM}$
NEUTRAL SHEET
35
30
25
20
15
10
RAD
9
10
11
12
MAY 1964

Figure 22

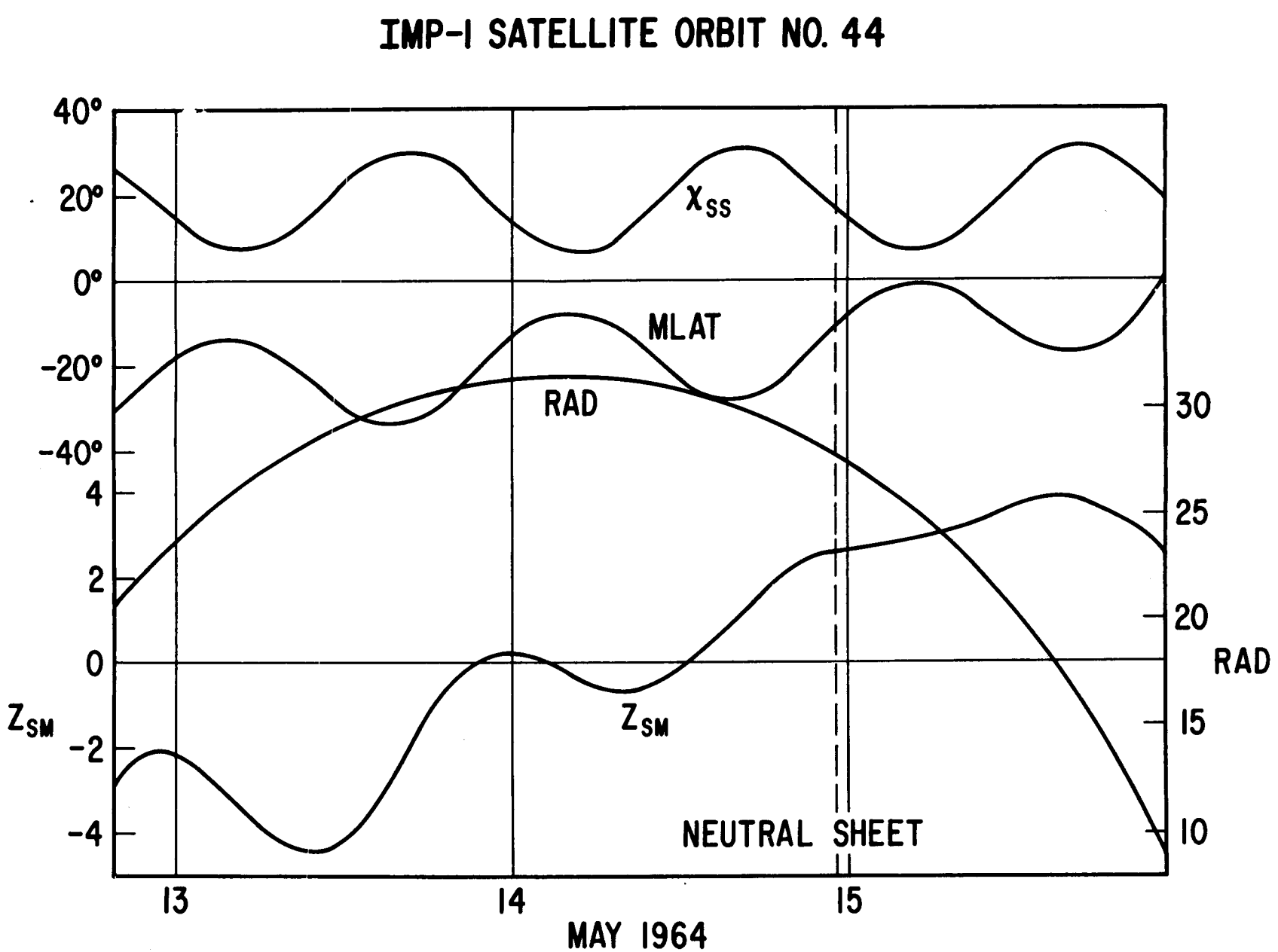
IMP-I SATELLITE ORBIT NO. 44
40°
20°
0°
-20°
-40°
4
2
0
-2
-4
$Z_{SM}$
$\chi_{SS}$
MLAT
RAD
$Z_{SM}$
NEUTRAL SHEET
30
25
20
15
10
RAD
13
14
15
MAY 1964

Figure 24

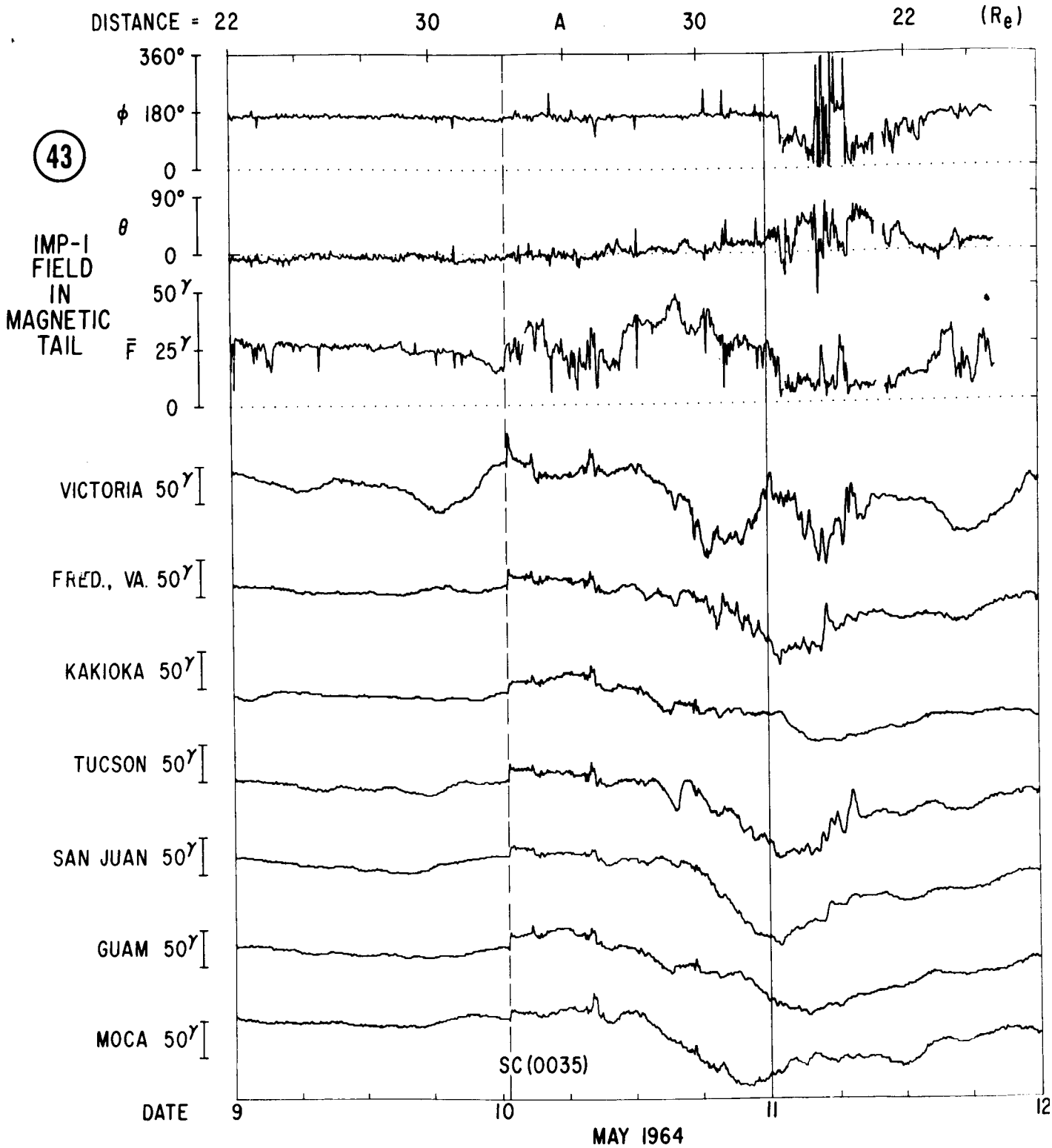
DISTANCE = 22
30
A
30
22
(Re)
360°
φ 180°
0
90°
θ
0
50γ
F 25γ
0
43
IMP-I FIELD IN MAGNETIC TAIL
VICTORIA 50γ
FRED., VA. 50γ
KAKIOKA 50γ
TUCSON 50γ
SAN JUAN 50γ
GUAM 50γ
MOCA 50γ
SC (0035)
DATE
9
10
11
12
MAY 1964

Figure 23

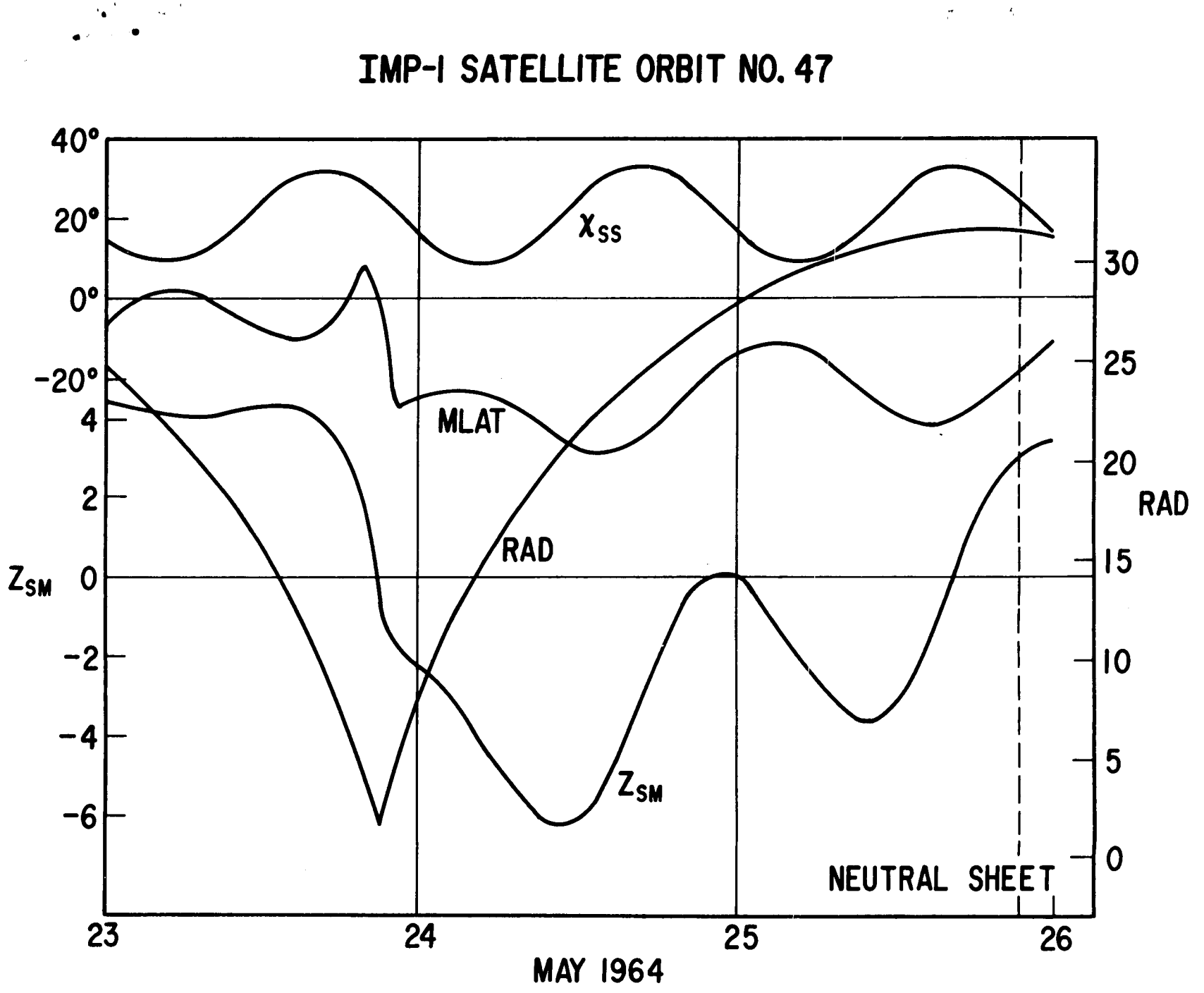
IMP-I SATELLITE ORBIT NO. 47
40°
20°
0°
-20°
4
2
0
-2
-4
-6
$Z_{SM}$
$\chi_{SS}$
MLAT
RAD
$Z_{SM}$
NEUTRAL SHEET
30
25
20
15
10
5
0
RAD
23
24
25
26
MAY 1964

Figure 26

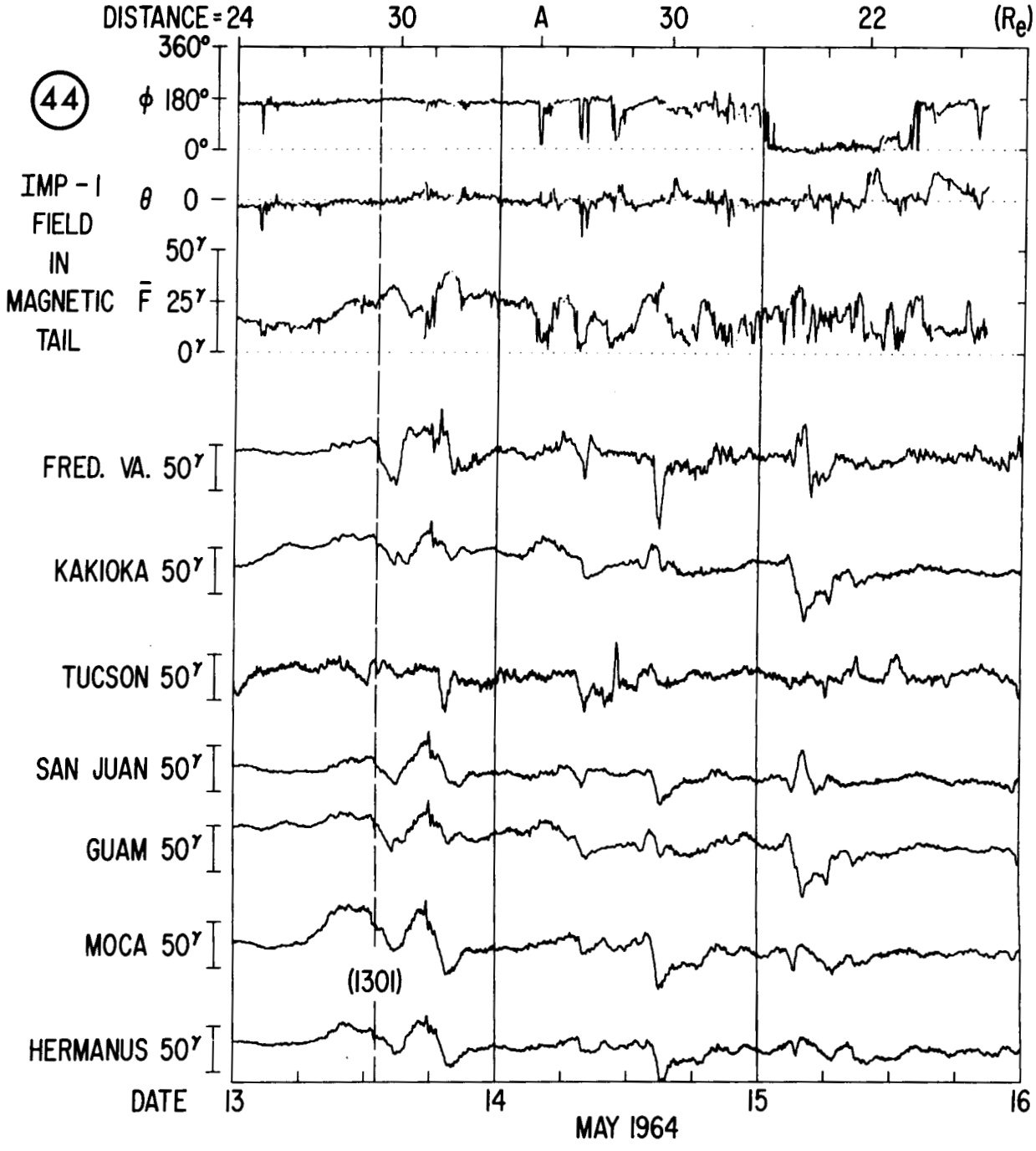
DISTANCE = 24
30
A
30
22
(Re)
360°
44
φ 180°
0°
IMP - I
FIELD
IN
MAGNETIC
TAIL
θ 0 -
50γ
F 25γ
0γ
FRED. VA. 50γ
KAKIOKA 50γ
TUCSON 50γ
SAN JUAN 50γ
GUAM 50γ
MOCA 50γ
(1301)
HERMANUS 50γ
DATE
13
14
15
16
MAY 1964

Figure 25

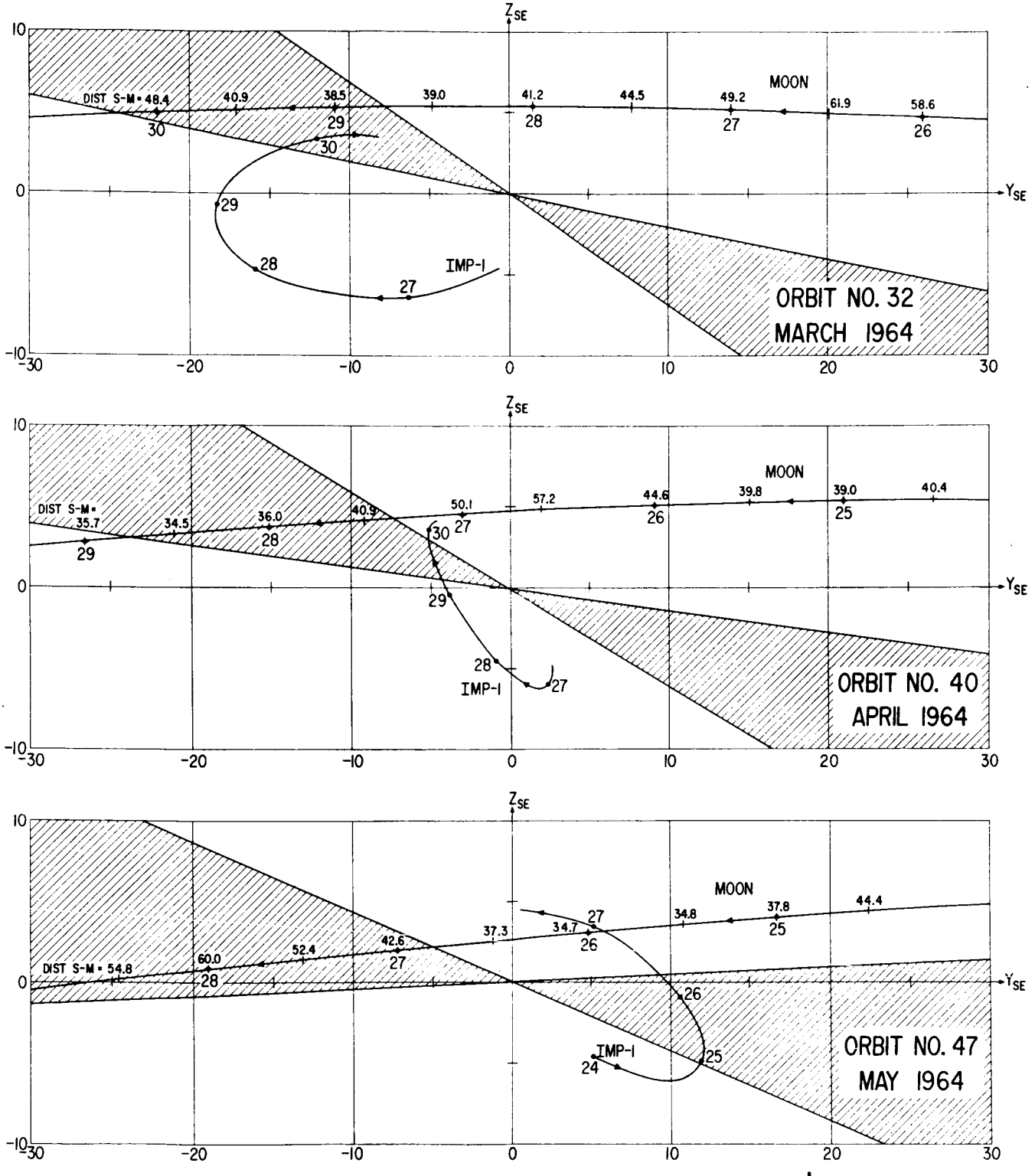


RELATIVE POSITION OF IMP-I & MOON IN EARTH'S TAIL

Figure 28

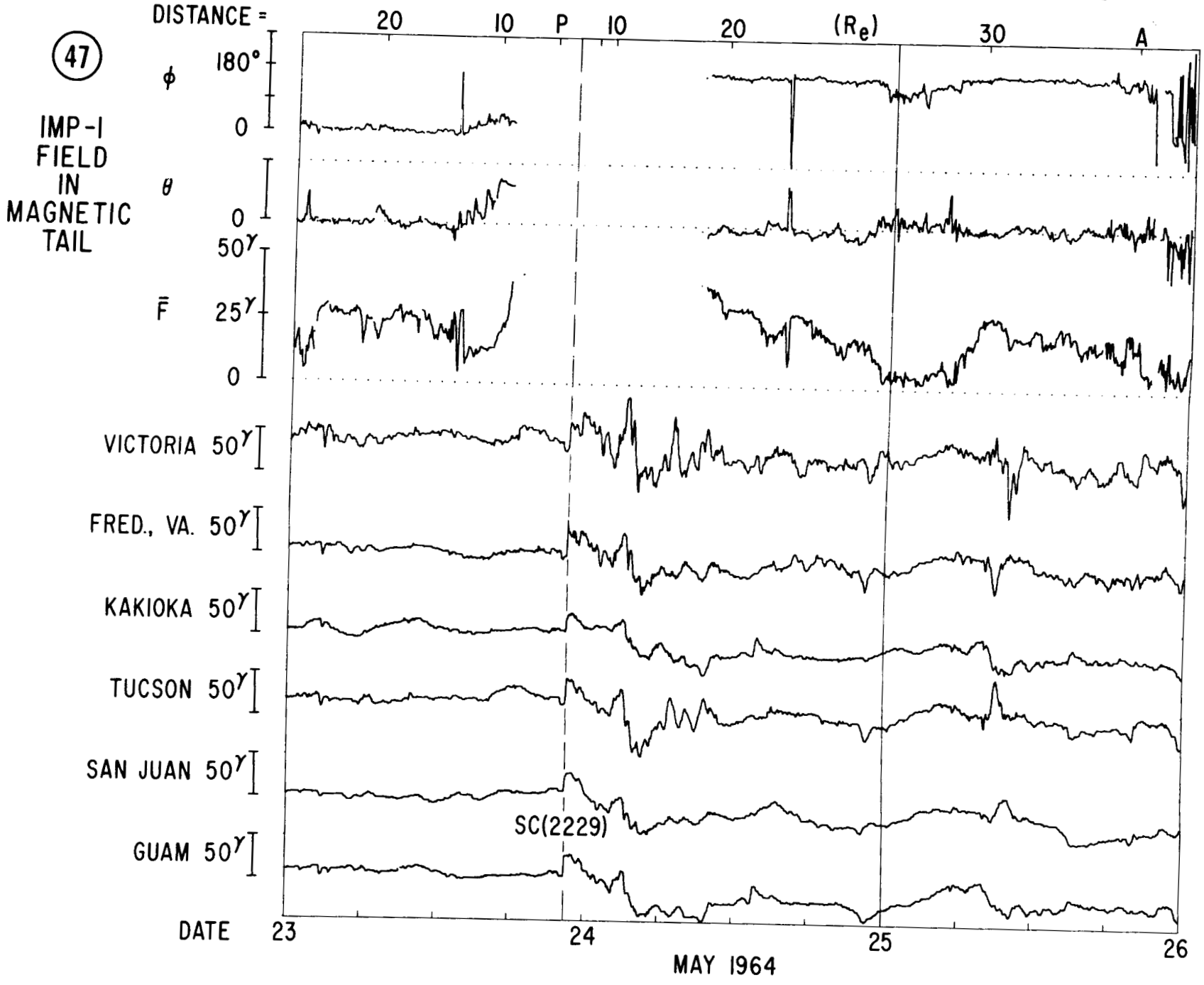
47
IMP-I FIELD IN MAGNETIC TAIL
DISTANCE =
20
10
P
10
20
(Re)
30
A
φ
180°
0
θ
0
50γ
F̄
25γ
0
VICTORIA 50γ
FRED., VA. 50γ
KAKIOKA 50γ
TUCSON 50γ
SAN JUAN 50γ
SC(2229)
GUAM 50γ
DATE
23
24
25
26
MAY 1964

Figure 27